West lake workshop on nuclear physics 2024

Imaging nuclear structure of atomic nuclei in high-energy nuclear collisions

Chunjian Zhang

Fudan University

10.18-20, 2024, Zhejiang University

Outline

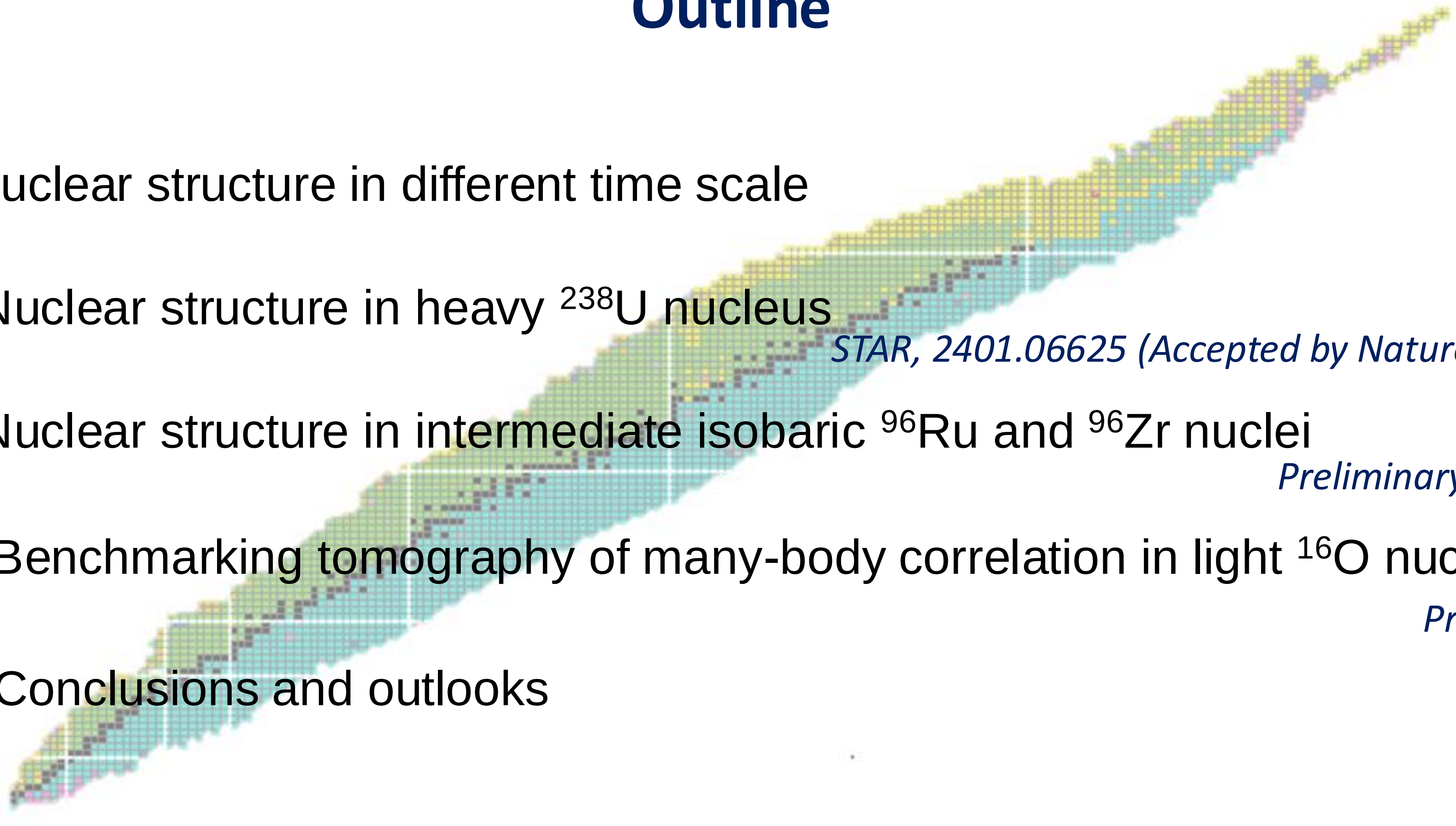

I. Nuclear structure in different time scale

II. Nuclear structure in heavy ^{238}U nucleus

STAR, 2401.06625 (Accepted by Nature)

II. Nuclear structure in intermediate isobaric ^{96}Ru and ^{96}Zr nuclei

Preliminary results

III. Benchmarking tomography of many-body correlation in light ^{16}O nucleus

Preliminary results

IV. Conclusions and outlooks

I. Nuclear structure in different time scales

The power of imaging

First-ever image of a black hole

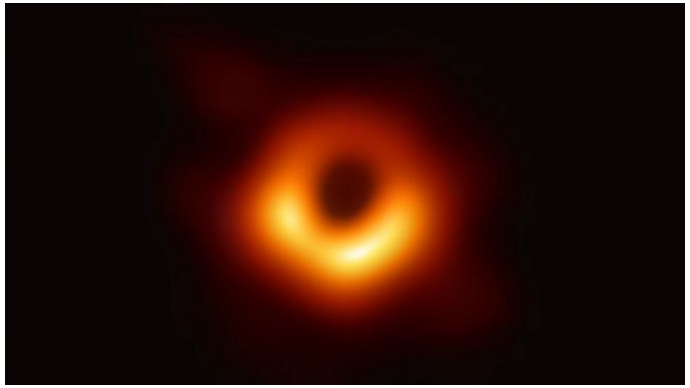

MRI CT image

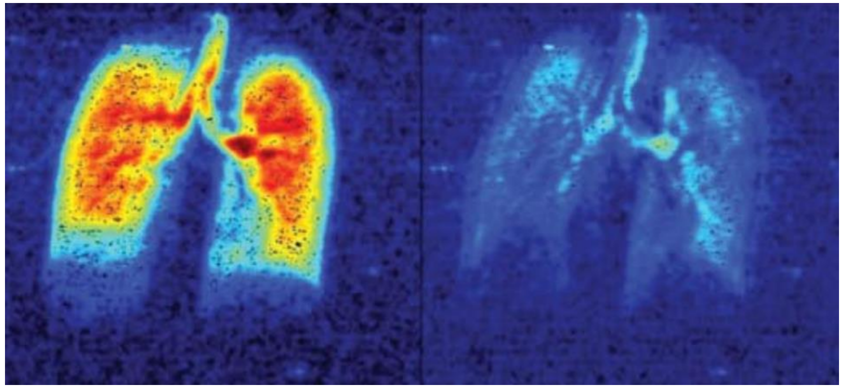

Image of electrons at attosecond

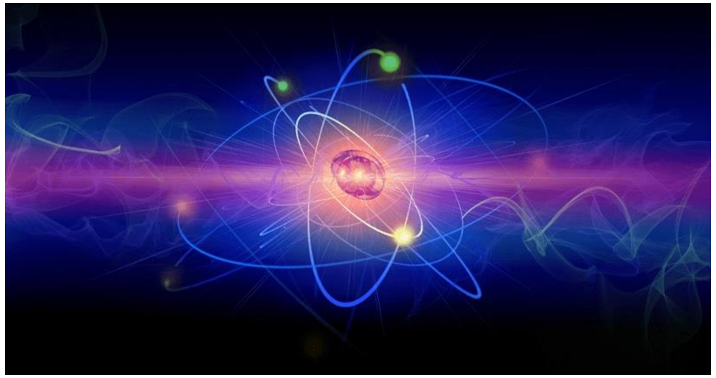

Astronomical scale → microscopic scale

Imaging: one of the scientific methods to understand nature!

Collective structure of atomic nuclei

RepProgPhys76, 126301(2013)

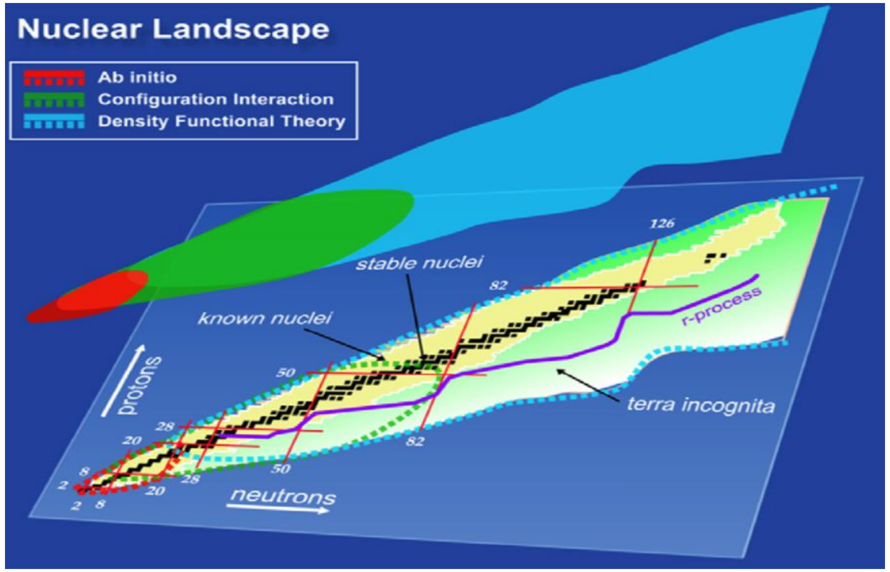

- Emergent phenomena of the many-body quantum system
  - Quadrupole/octupole/hexadecapole deformations
  - Clustering, halo, skin, bubble…
  - Non-monotonic evolution with *N* and Z

Quadrupole

S. Cwiok et al.,Nature433, 705(2005)

Octupole

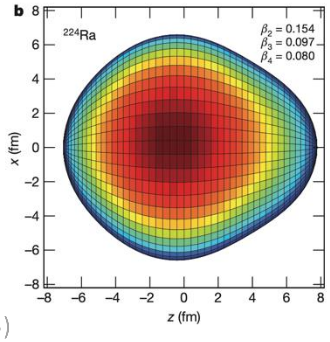

LP Gaffney et al., Nature497, 199(2013)

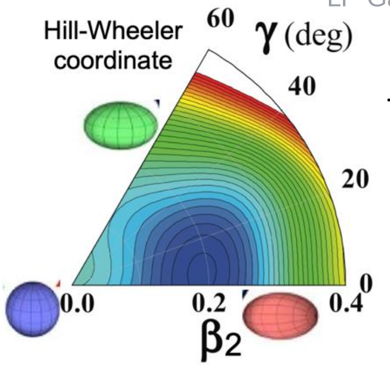

Triaxial spheroid

AN Andreyev et al., Nature405, 430(2000)

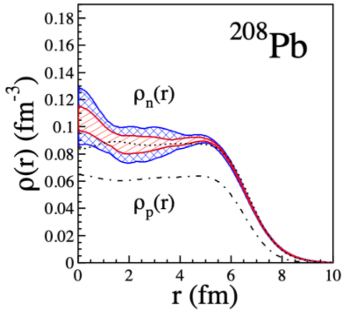

Neutron skin

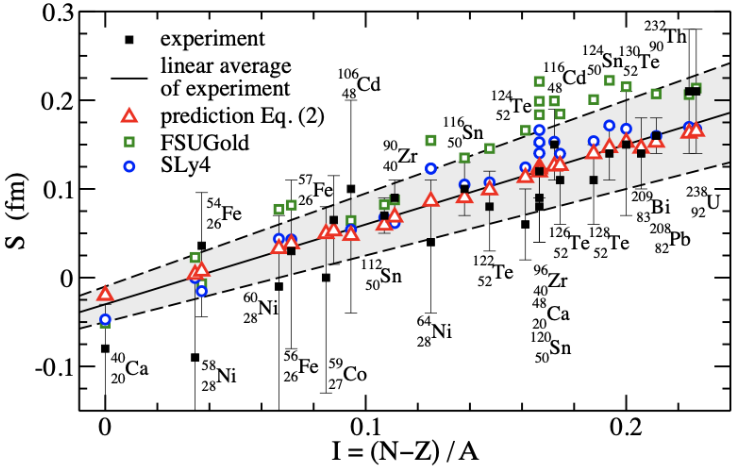

A. Trzcinska et al., PRL87, 082501(2001)
B. M. Centelles et al., PRL102, 122502(2009)

nucleonic clustering

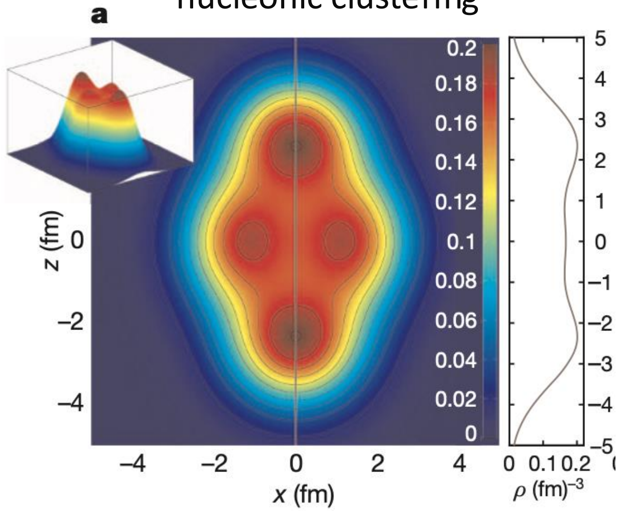

J.P. Ebran et al. Nature487, 341(2012)

Multi-stages in relativistic heavy-ion collisions

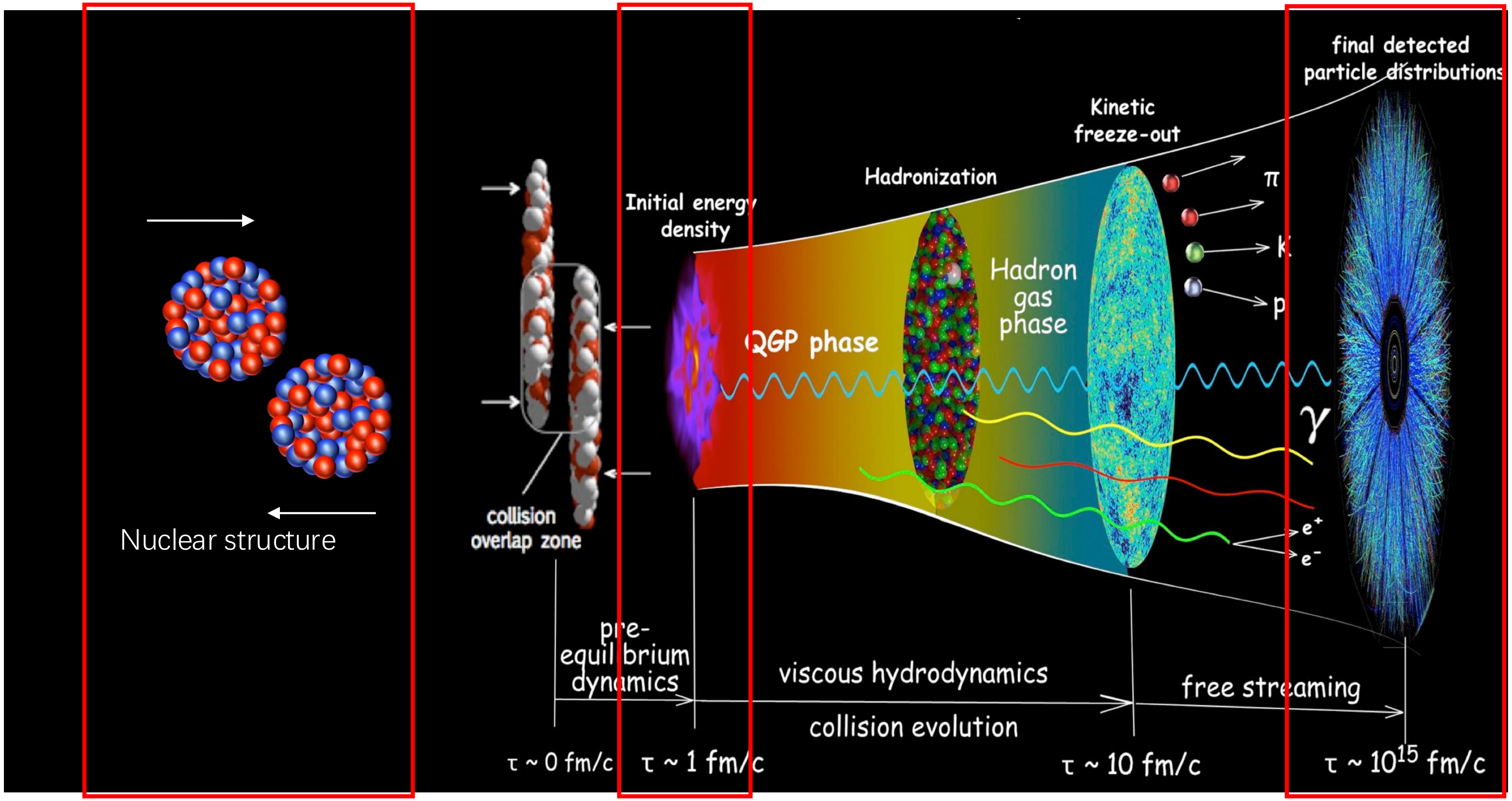

Multiple stage
/Complex dynamics

Hybrid multi-stage
Modeling with event-by
-event fluctuations

$$\rho(r,\theta,\phi) = \frac{\rho_0}{1+e^{(r-R(\theta,\phi))/a_0}}$$

$$e(x,y) \sim \begin{cases} T_A + T_B & N_{\text{part}} - \text{scaling}, p=1 \\ T_A T_B & N_{\text{coll}} - \text{scaling}, p=0, q=2 \\ \sqrt{T_A T_B} & \text{Trento default}, p=0 \\ \min\{T_A, T_B\} & \text{KLN model}, p \sim -2/3 \\ T_A + T_B + \alpha T_A T_B & \text{two-component model,} \\ & \text{similar to quark-glauber model} \end{cases}$$

$$T \propto \left(\frac{T_A^p + T_B^p}{2}\right)^{q/p}$$

Collective flow assisted nuclear structure imaging

Nuclear structure

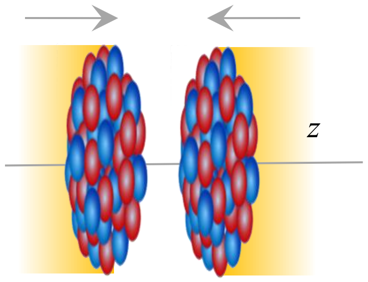

Imaging

Initial state

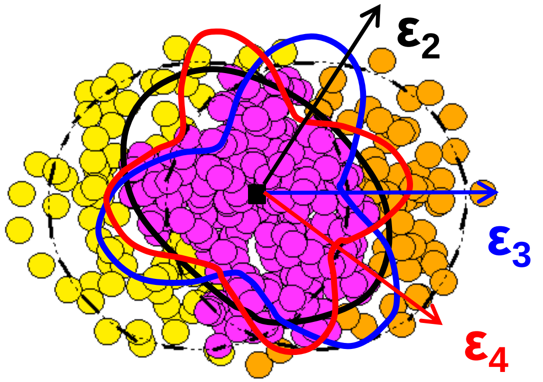

$F = -\nabla P(\epsilon)$

hydro-response

Final state

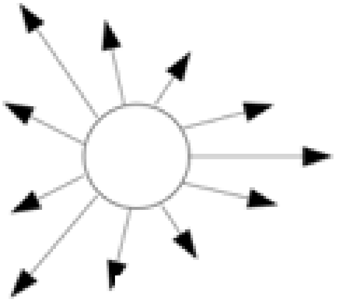

$$\rho(r,\theta,\phi) = \frac{\rho_0}{1 + e^{(r - R(\theta,\phi))/a_0}}$$

$$R(\theta,\phi) = R_0(1 + \beta_2[\cos\gamma Y_{2,0}(\theta,\phi) + \sin\gamma Y_{2,2}(\theta,\phi)] + \beta_3 Y_{3,0}(\theta,\phi))$$

- β_2 → Quadrupole deformation
- β_3 → Octupole deformation
- γ → Triaxiality
- a_0 → Surface diffuseness
- R_0 → Nuclear size

Many-body correlations

?

Initial Size: $R_\perp^2 \propto \langle r_\perp^2 \rangle$

Initial Shape: $\mathcal{E}_n \propto \langle r_\perp^n e^{in\phi} \rangle$

R_0 $\quad a_0 \quad$ β_n

Radial Flow **Anisotropic Flow**

$$\frac{d^2N}{d\phi dp_T} = N(p_T)\left(\sum_n V_n e^{-in\phi}\right)$$

$N_{ch} \propto N_{part}$ $\quad \frac{\delta[p_T]}{[p_T]} \propto -\frac{\delta R_\perp}{R_\perp}$ $\quad V_n \propto \mathcal{E}_n$

High energy: Large multiplicity and boost invariance; approximate linear response in each event

- Constrain the initial condition by comparing nuclei with known structure properties.
- Reveal novel properties of nuclei by leveraging known hydrodynamic response.
- Study the unknown nuclear structure by heavy-ion collisions.

Low-energy spectroscopy vs high-energy snapshot method

- Intrinsic frame shape not directly visible in lab frame
  --Mainly inferred from non-invasive spectroscopy methods.

STAR, 2401.06625
(Accepted by Nature)

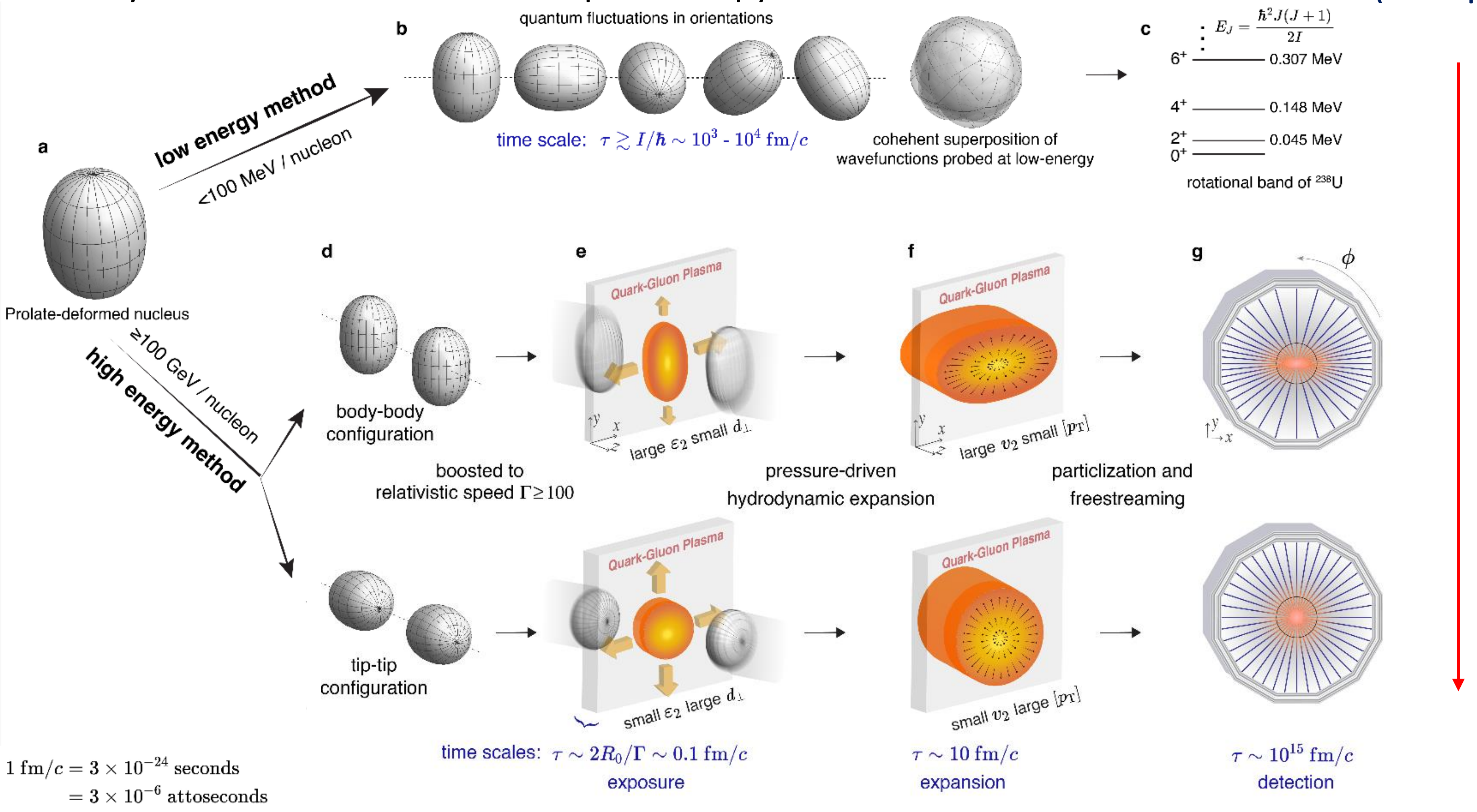

Energy/time scales

- Shape-frozen like snapshot in nuclear crossing (10^{-25}s << rotational time scale 10^{-21}s)
  --probe entire mass distribution in the intrinsic frame via multi-point correlations.

Snapshot imaging = tracing the intrinsic nuclear structure?

"…figuring out a pocket watch by smashing two together and observing the flying debris"

— Richard Feynman

Short-time scale imaging could see detailed shapes?

STAR detector at Brookhaven National Laboratory

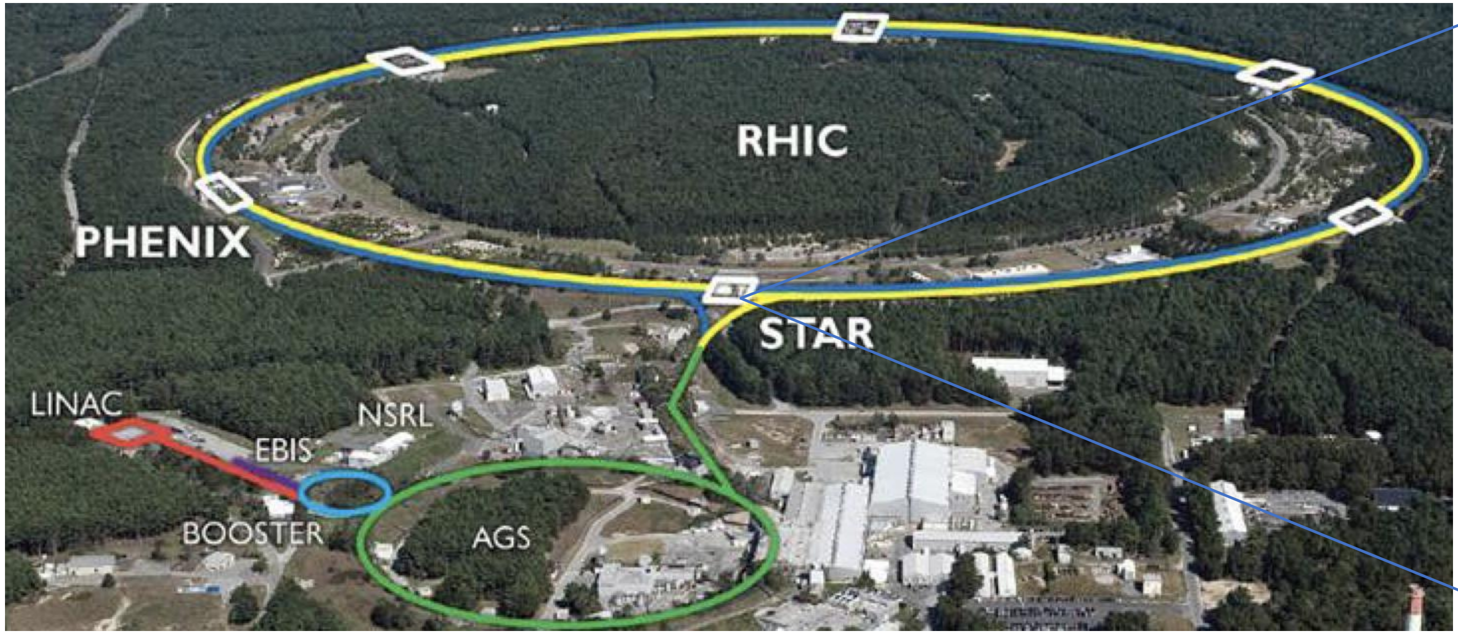

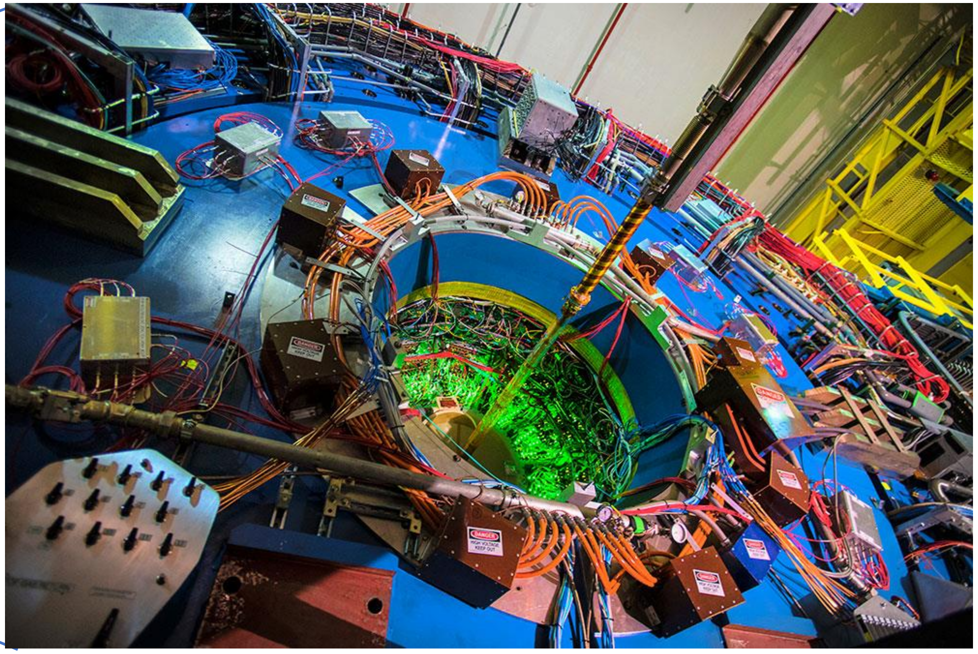

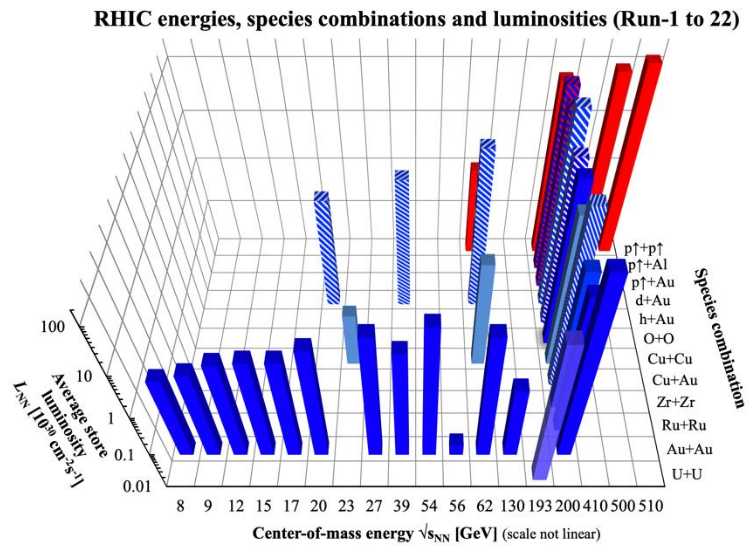

STAR detector provides

1) large, uniform acceptance at mid-rapidity
2) vast number of emitted final state hardons
3) capability to access nuclear structures in U+U, Au+Au, Ru+Ru, Zr+Zr, and O+O collisions…

II. Nuclear structure in heavy ^{238}U nucleus

$$\rho(r,\theta,\phi) = \frac{\rho_0}{1+e^{(r-R(\theta,\phi))/a_0}}$$

$$R(\theta,\phi) = R_0(1+\beta_2[\cos\gamma Y_{2,0}(\theta,\phi)+\sin\gamma Y_{2,2}(\theta,\phi)]+\beta_3 Y_{3,0}(\theta,\phi)+\beta_4 Y_{4,0}(\theta,\phi))$$

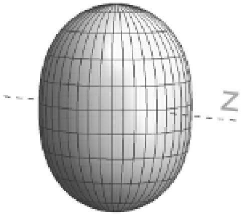

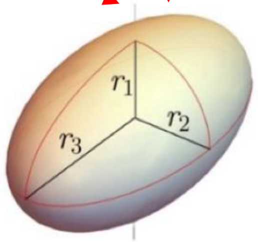

W. Ryssens, G. Giacalone, B. Schenke and C. Shen, PRL130, 212302(2023)

DFT calculations predict a slightly small WS deformation $\beta_{2U} \approx 0.28 \rightarrow \beta_{2U,WS} \approx 0.25$

corresponding to a larger volume deformation in presence of $\boldsymbol{\beta}_{4U}$~0.1 $\beta_{2,\mathrm{body}} = \frac{4\pi}{3R_0^2 A}\int d^3r\rho(\mathbf{r})r^2Y_{20}$

Low-energy estimate with rigid rotor assumption from B(E2) data $\beta_{2,\mathrm{LD}} = \frac{4\pi}{5R_0^2 Z}\sqrt{\frac{B(\mathrm{E2})}{e^2}}$

$\beta_{2U,LD} = 0.287 \pm 0.007 \quad \gamma_{U,LD} = 6^\circ - 8^\circ$

B. Pritychenko et al., J.ADT.107, 1(2016)
C. Y. Wu et al., PRC54, 2356(1996)

Evidence of deformation from system comparison

Two particle correlator:

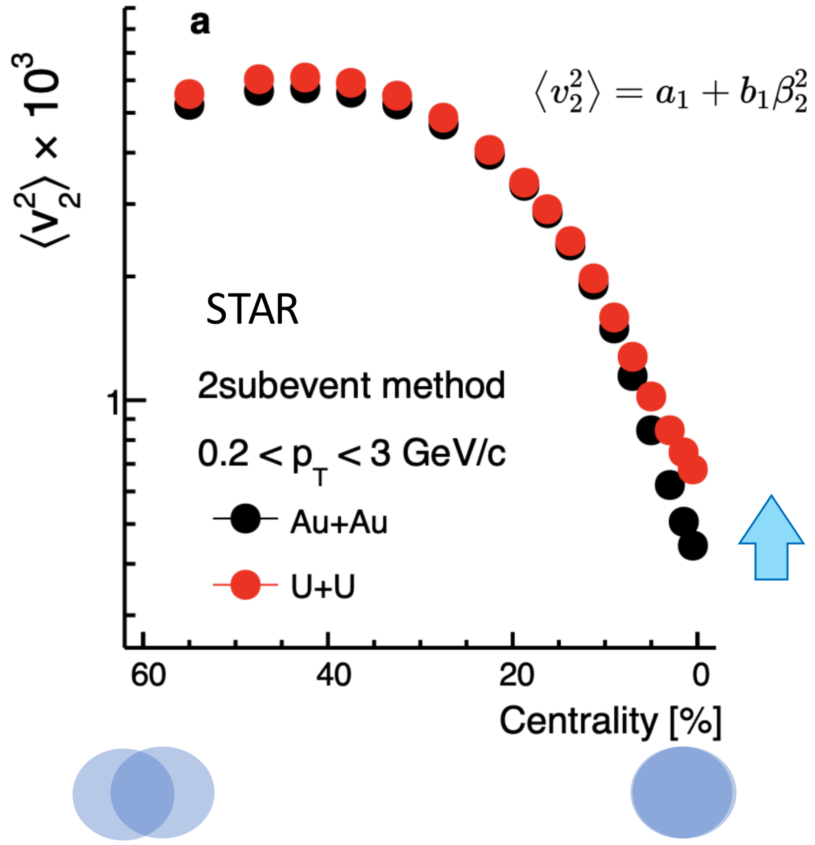

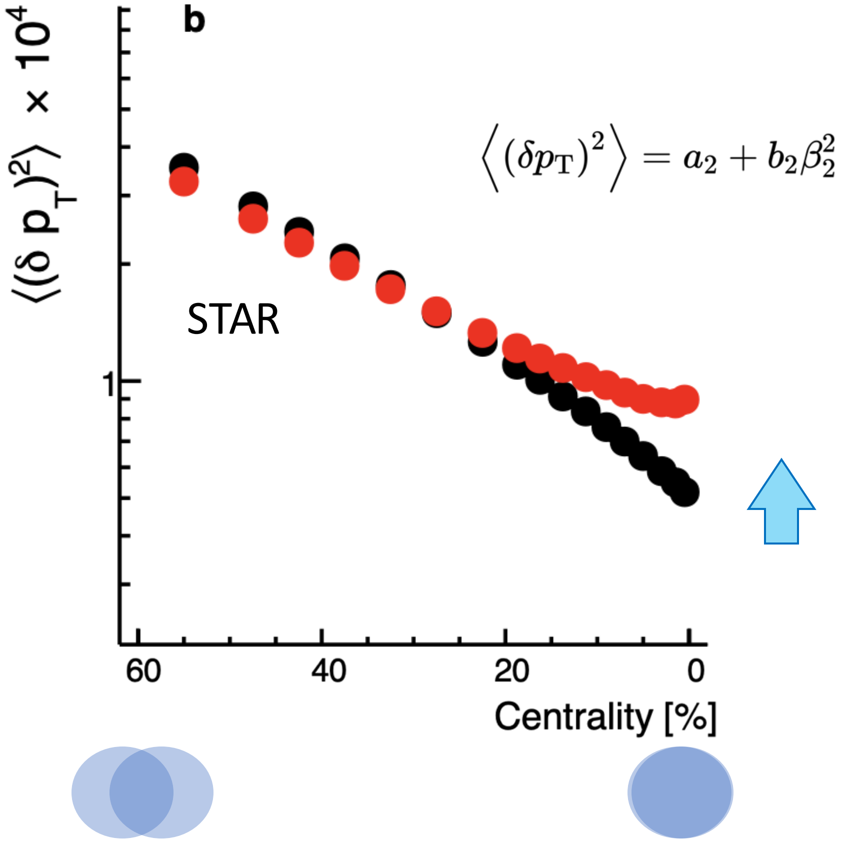

Elliptic flow and size fluctuation are enhanced by the nuclear deformation effect.

Model: G. Giacalone, J.Jia and C. Zhang, PRL127, 242301(2021)

Reflecting the initial state from the nuclear geometry

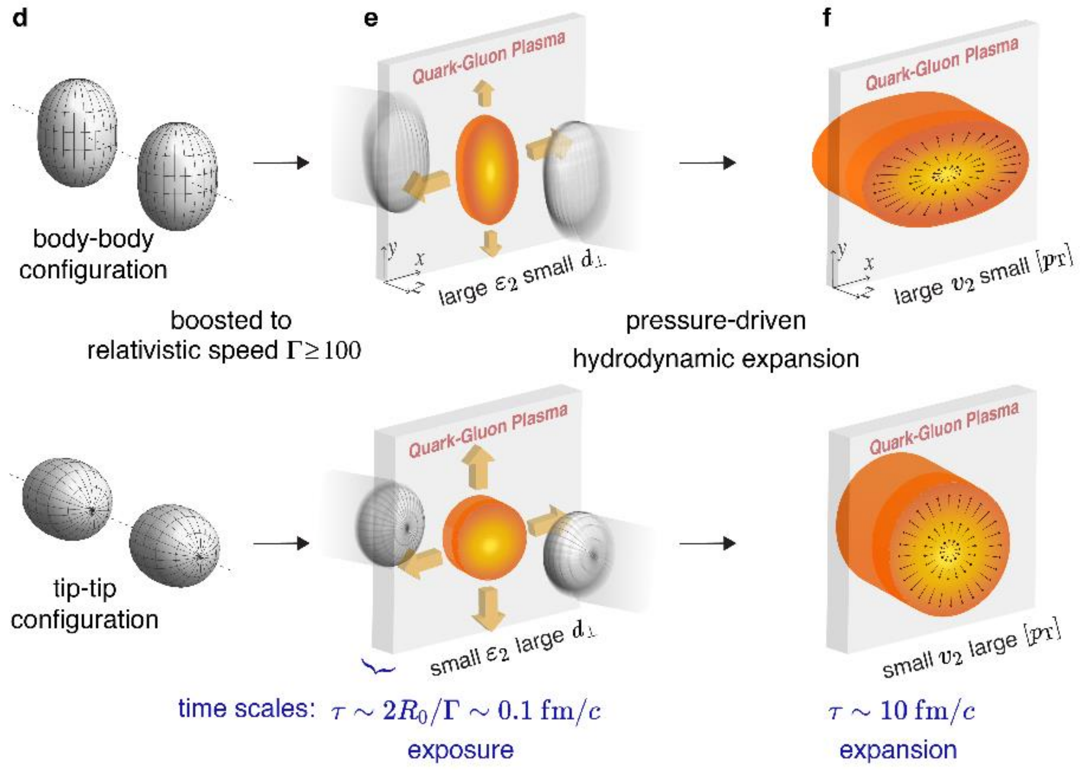

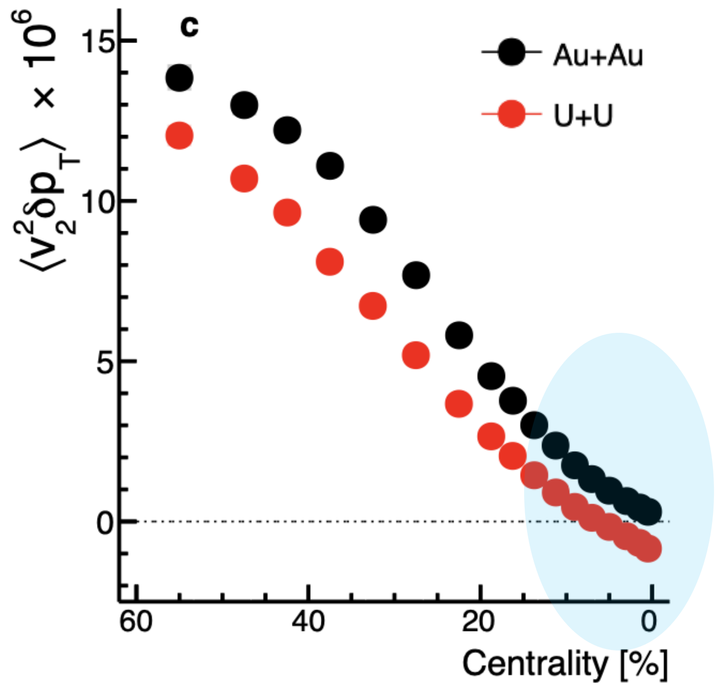

v_n-$[p_T]$ three particle correlator

$$\mathrm{cov}\left(v_n^2, [p_T]\right) \equiv \left\langle \frac{\sum_{i\neq j\neq k} w_i w_j w_k e^{in\phi_i} e^{-in\phi_j} \left(p_{T,k} - \langle\langle p_T \rangle\rangle\right)}{\sum_{i\neq j\neq k} w_i w_j w_k} \right\rangle_{\mathrm{evt}}$$

$$[p_T] \equiv \frac{\sum_i w_i p_{T,i}}{\sum_i w_i}, \langle\langle p_T \rangle\rangle \equiv \langle [p_T] \rangle_{\mathrm{evt}}$$

w_i is track weight

- $\boldsymbol{\varepsilon}_2$ and R are influenced by the quadrupole deformation β_2
- $\langle p_T \rangle \sim 1/R$ and $v_2 \propto \boldsymbol{\varepsilon}_2$: $\left\langle \epsilon_n^2 \frac{1}{R} \right\rangle \rightarrow \left\langle v_n^2\, p_T \right\rangle$

deformation contributes to anticorrelation between v_2 and $\langle p_T \rangle$

P. Bozek, PRC93, 044908(2016)

Sign-change in U+U in central collisions; Au+Au remains positive

Extracting shape of ^{238}U: quadrupole deformation and triaxiality

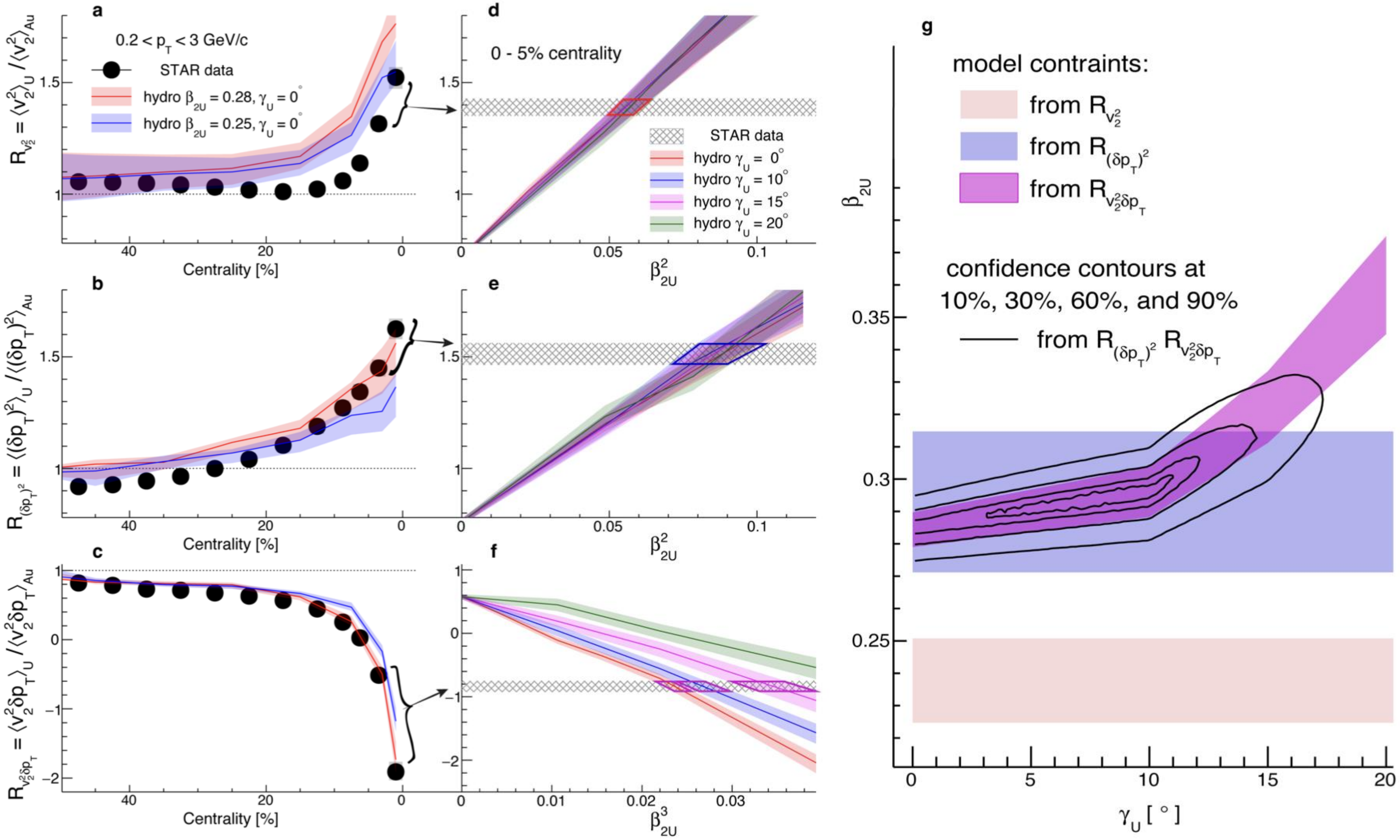

Achieves a better description of ratios in UCC region

$$\langle v_2^2 \rangle = a_1 + b_1 \beta_2^2$$

$$\left\langle (\delta p_{\mathrm{T}})^2 \right\rangle = a_2 + b_2 \beta_2^2$$

$$\langle v_2^2 \delta p_{\mathrm{T}} \rangle = a_3 - b_3 \beta_2^3 \cos(3\gamma)$$

Constraints on β_2 of ^{238}U from data comparison with hydro

$$\beta_{2\mathrm{U}} = 0.297 \pm 0.013$$

$$\gamma_U = 8.6^\circ \pm 4.8^\circ$$

Understanding the nuclear deformation in the shorter time scale.

A novel way to quantify the shape of ^{238}U.

Sanity/systematic check #1 : viscosity effect

Ratios cancel the viscosity effects.

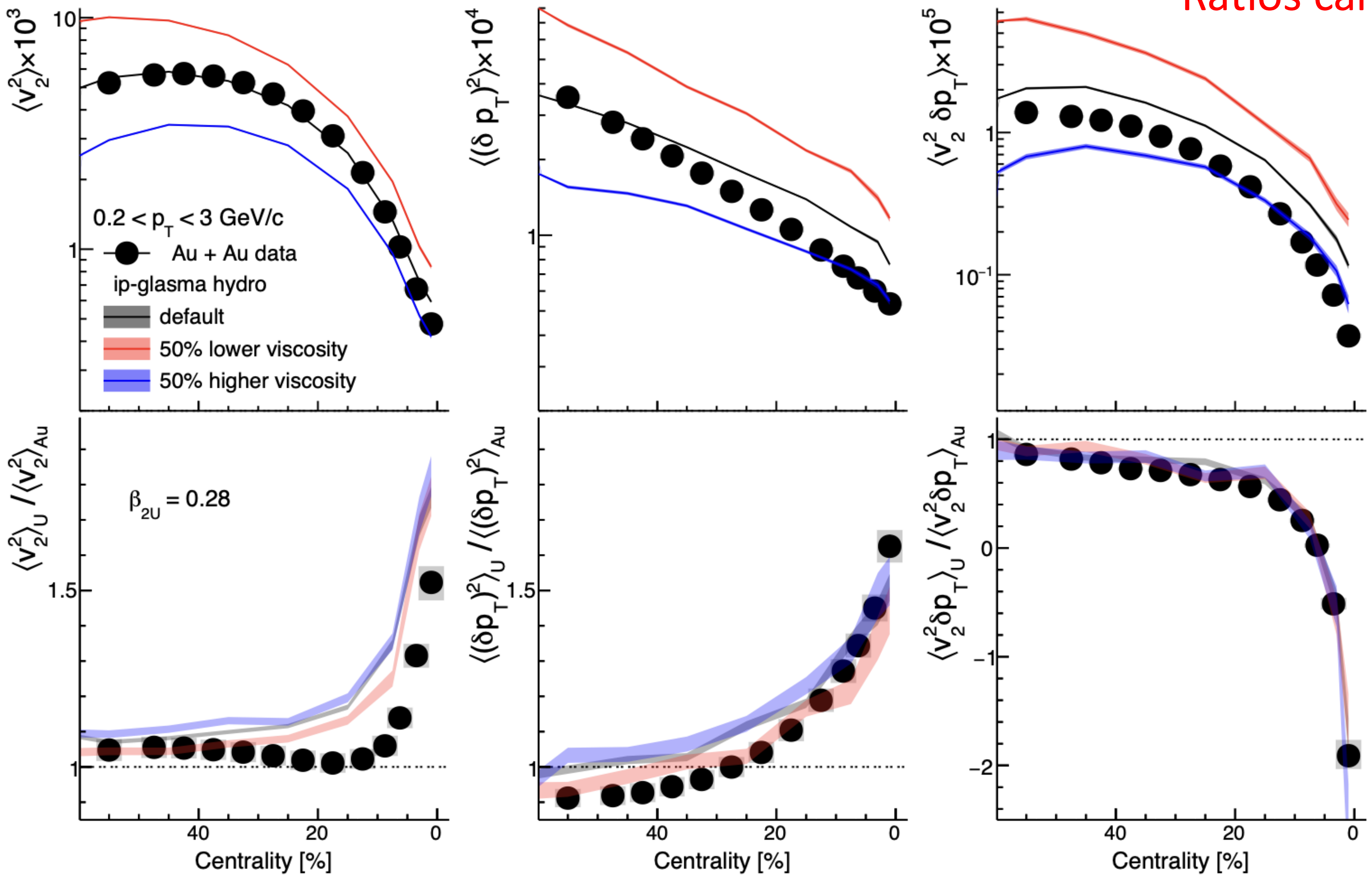

Sanity/systematic check #2 : nuclear parameters effect

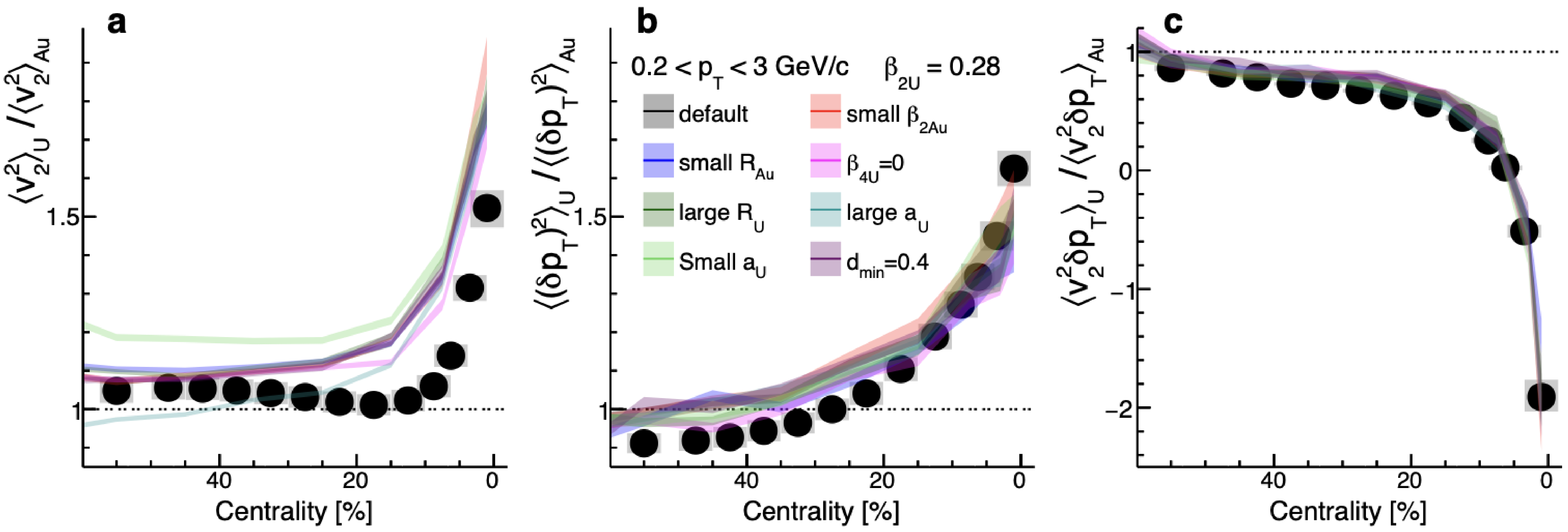

Effect from nuclear parameters are smaller and included as model systematics.

Sanity/systematic check #3 : different hydrodynamic models

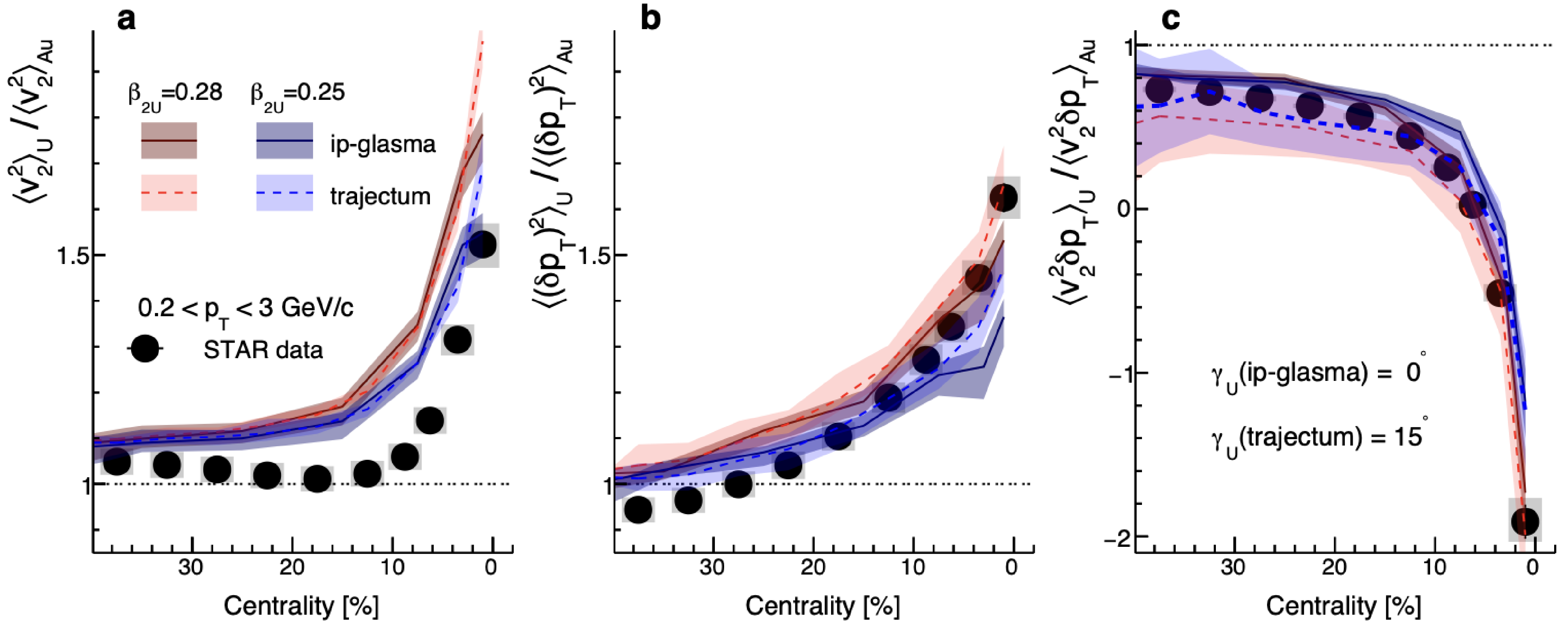

Other hydrodynamics model (Trajectum) also shows rather consistent extractions even if it was not tuned to RHIC data.

check #1#2#3 of model systematics sources are included in the experimental paper.

Mean transverse momentum $[p_T]$ fluctuations

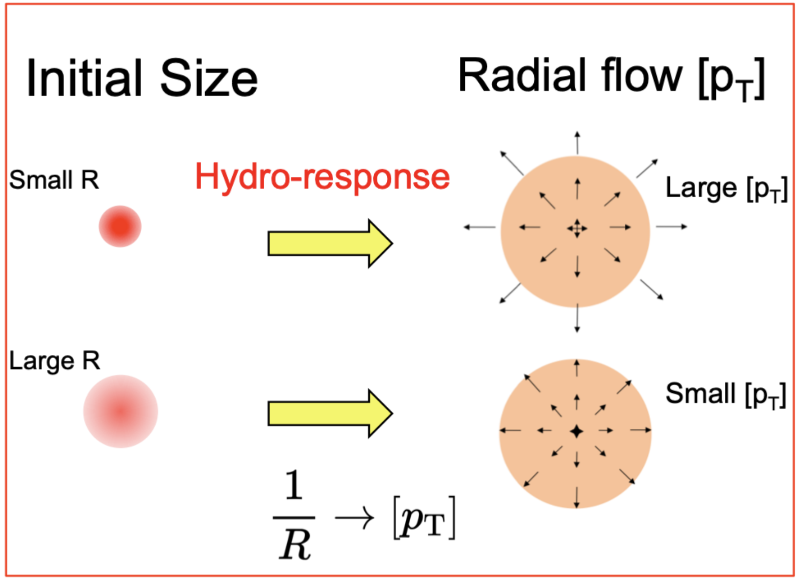

$$\begin{array}{c} S_A = S_B \\ R_A < R_B \end{array} \Longrightarrow T_A > T_B \Longrightarrow \overline{p}_{t,A} > \overline{p}_{t,B}$$

Same total energy deposition:
Smaller transverse size,
Stronger radial expansion.

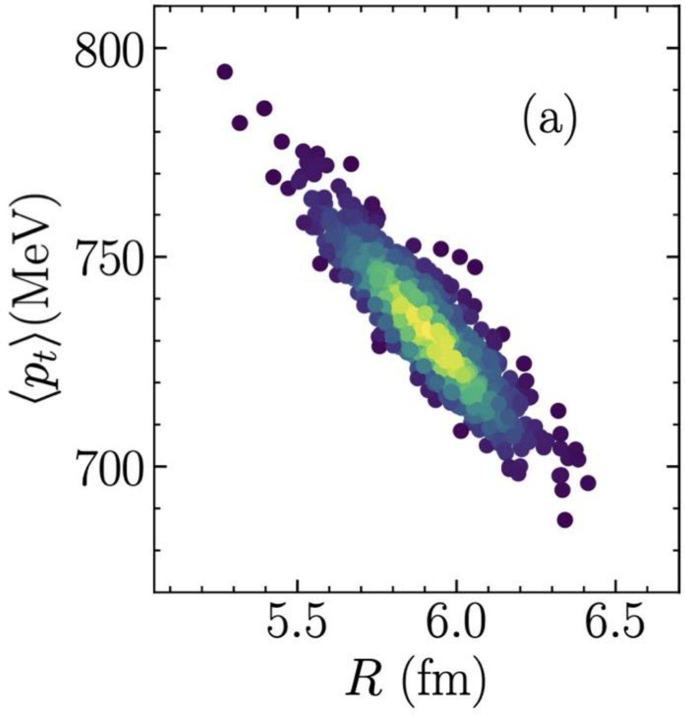

$$\delta[p_T] \propto -\delta R \propto \delta d_\perp$$

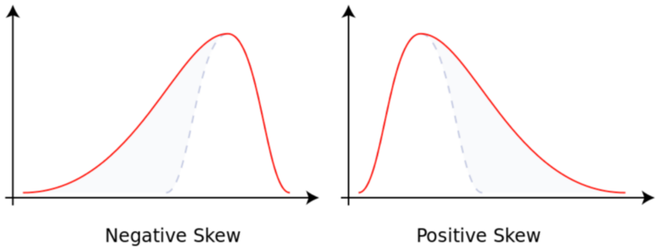

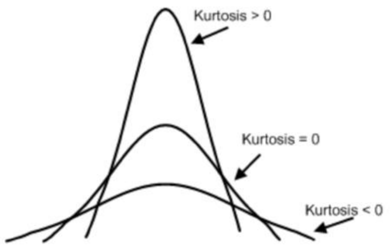

J. Jia, PRC105, 044905(2021)

Mean $\frac{\delta[p_T]}{[p_T]} \propto \frac{\delta d_\perp}{d_\perp} \propto \beta_2$

Variance $\left\langle\left(\frac{\delta[p_T]}{[p_T]}\right)^2\right\rangle \propto \left\langle\left(\frac{\delta d_\perp}{d_\perp}\right)^2\right\rangle \propto \beta_2^2$

Skewness $\left\langle\left(\frac{\delta[p_T]}{[p_T]}\right)^3\right\rangle \propto \left\langle\left(\frac{\delta d_\perp}{d_\perp}\right)^3\right\rangle \propto cos(3\gamma)\beta_2^3$

Kurtosis $\left\langle\left(\frac{\delta[p_T]}{[p_T]}\right)^4\right\rangle - 3\left\langle\left(\frac{\delta[p_T]}{[p_T]}\right)^2\right\rangle^2 \propto \left\langle\left(\frac{\delta d_\perp}{d_\perp}\right)^4\right\rangle - 3\left\langle\left(\frac{\delta d_\perp}{d_\perp}\right)^2\right\rangle^2 \propto -\beta_2^4$

Event-by-event $[p_T]$ fluctuations also reflect the deformation of colliding nuclei

[p_T] fluctuations and comparisons to hydro model

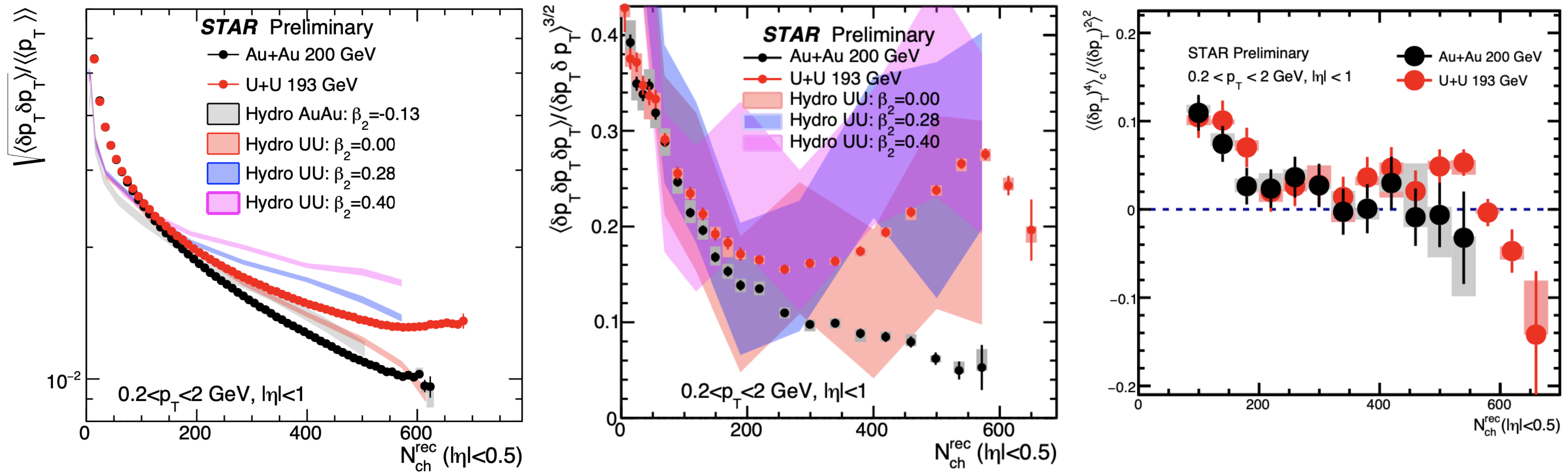

Au+Au: variance and skewness follow independent source scaling $1/N_s^{n-1}$ within power-law decrease

U+U: large enhancement in normalized variance and skewness and sign-change in normalized kurtosis

⟶ size fluctuations enhanced

The nuclear deformation role is further confirmed by hydro calculations.

Hydro: private calculations from Bjoern Schenke and Chun Shen

[p_T] fluctuations also serve as a good observable to explore the role of nuclear deformation.

Other interesting questions remained:

1. More new observables also need to be investigated.

2. Current calculations are in 2D transverse profile, but how 3D will be?

   Model: C. Zhang, S. Huang and J.Jia, 2405.08749
   J. Jia, S. Huang, C. Zhang and S. Bhatta, 2408.16006

3. High-order deformations & ”soft” or “rigid” Triaxiality.

   Model: H. Xu, J. Zhao and F. Wang, PRL132, 262301(2024)
   Z. Wang, J. Chen, H. Xu and J. Zhao, 2405.09329
   A. Dimri, S. Bhatta, J. Jia, 2301.03556

4. Precise data-model comparisons and the accuracy of the initial state.

III. Structure of intermediate isobaric ^{96}Ru and ^{96}Zr nuclei

$$\rho(r,\theta,\phi) = \frac{\rho_0}{1+e^{(r-R(\theta,\phi))/a_0}}$$

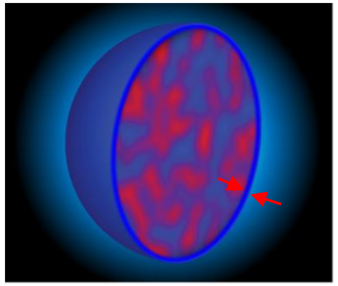

$$R(\theta,\phi) = R_0(1+\beta_2[\cos\gamma Y_{2,0}(\theta,\phi)+\sin\gamma Y_{2,2}(\theta,\phi)]+\beta_3 Y_{3,0}(\theta,\phi))$$

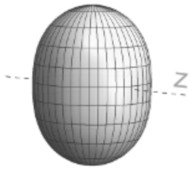

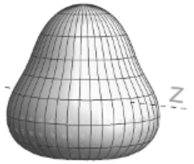

Lower energies experimental measurement

$$\beta_2 = \frac{4\pi}{3ZR_0^2}\sqrt{\frac{B(E2)\uparrow}{e^2}} \qquad \beta_3 = \frac{4\pi}{3ZR_0^3}\sqrt{\frac{B(E3)\uparrow}{e^2}}$$

	β_2	$E_{2_1^+}$ (MeV)	β_3	$E_{3_1^-}$ (MeV)
^{96}Ru	0.154	0.83	-	3.08
^{96}Zr	0.062	1.75	0.202,0.235,0.27	1.90

Evidence of static octupole moments at low energies is rather sparse.

Pear-shaped nuclei enable new physics searches?

US Long Range Plan 2023

Sidebar 6.2 Radioisotope harvesting at FRIB for fundamental physics

The Facility for Rare Isotope Beams (FRIB) will yield the discovery of new, exotic isotopes and the measurement of reaction rates for nuclear astrophysics, and will produce radioactive isotopes that can be used for a broad range of applications, including medicine, biology, and fundamental physics.

Converting waste to wealth

Radioisotopes at FRIB are produced via fragmentation when accelerated ion beams interact with a thin target. Several isotopes, including those previously unobserved, across the entire periodic table will be produced in practical quantities for the first time in the water beam dump at the FRIB accelerator. The Isotope Harvesting Project provides a new opportunity to collect these isotopes, greatly enhancing their yield and real-time availability to enable a broad spectrum of research across multiple scientific disciplines. Isotopes will be extracted from the beam dump and chemically purified using radiochemistry techniques in a process called harvesting. Harvesting operates commensally, therefore providing additional opportunities for science.

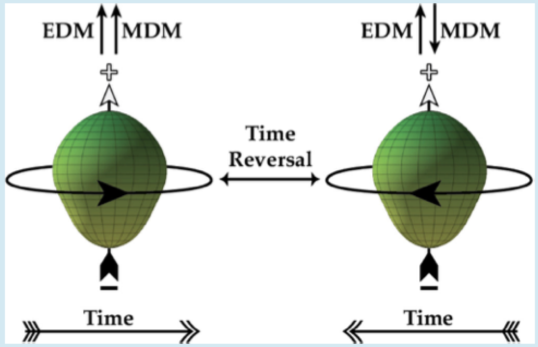

Figure 1. A pear-shaped nucleus spins counterclockwise or clockwise, depending on the direction of time. [S47]

Pear-shaped nuclei enable new-physics searches

With uranium-238 ion beams, these methods can produce heavy, pear-shaped nuclei that can be used to search for violations of fundamental symmetries that would signal new forces in nature. For example, a nonzero permanent electric dipole moment (EDM) would break parity and time-reversal symmetries. Figure 1 shows a pear-shaped nucleus spinning under applied electric and magnetic fields. Its magnetic dipole moment (MDM) is nonzero, and if its EDM is also nonzero, then its spin-precession rate changes if the direction of time is reversed. Heavy, pear-shaped nuclei can greatly amplify the sensitivity to a nonzero EDM and complement neutron EDM studies. Pear-shaped isotopes such as radium-225 and protactinium-229 will be produced in abundance at FRIB, and their EDM effects can be further enhanced by using them to form polar molecules, which can then be probed using cutting-edge laser techniques. The unique sensitivity of these experiments opens otherwise inaccessible windows on new physics.

EDMs are very small and difficult to measure.

Higher sensitivity via Schiff nuclear moments in heavy nuclei

-> Octupole deformation enhancements

Hunt for the no neutrinos

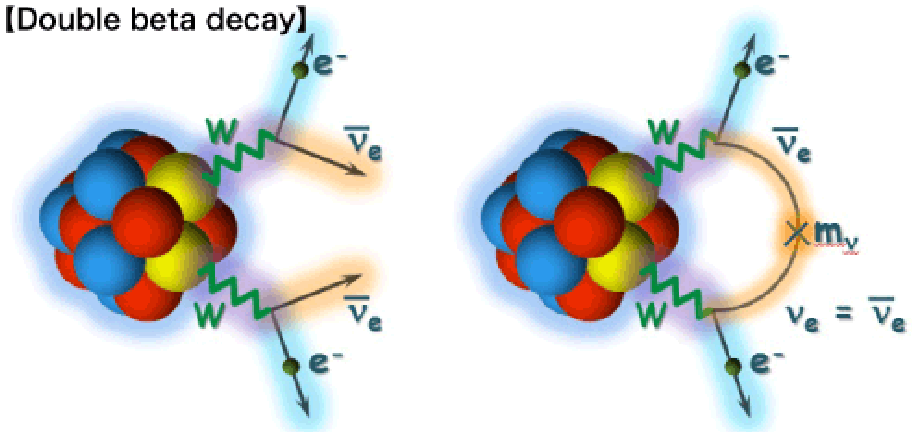

Double beta decay which emits anti-neutrinos

Neutrinoless double beta decay

Isotope	$T^{0\nu}_{1/2}$ ($\times 10^{25}$ y)	$\langle m_{\beta\beta}\rangle$ (eV)	Experiment	Reference
^{48}Ca	$> 5.8 \times 10^{-3}$	$< 3.5 - 22$	ELEGANT-IV	(157)
^{76}Ge	> 8.0	$< 0.12 - 0.26$	GERDA	(158)
	> 1.9	$< 0.24 - 0.52$	MAJORANA DEMONSTRATOR	(159)
^{82}Se	$> 3.6 \times 10^{-2}$	$< 0.89 - 2.43$	NEMO-3	(160)
^{96}Zr	$> 9.2 \times 10^{-4}$	$< 7.2 - 19.5$	NEMO-3	(161)
^{100}Mo	$> 1.1 \times 10^{-1}$	$< 0.33 - 0.62$	NEMO-3	(162)
^{116}Cd	$> 1.0 \times 10^{-2}$	$< 1.4 - 2.5$	NEMO-3	(163)
^{128}Te	$> 1.1 \times 10^{-2}$	—	—	(164)
^{130}Te	> 1.5	$< 0.11 - 0.52$	CUORE	(124)
^{136}Xe	> 10.7	$< 0.061 - 0.165$	KamLAND-Zen	(165)
	> 1.8	$< 0.15 - 0.40$	EXO-200	(166)
^{150}Nd	$> 2.0 \times 10^{-3}$	$< 1.6 - 5.3$	NEMO-3	(167)

^{96}Zr with high-case rate, strong neutrino mass limiting ability

$$T^{0\nu}_{1/2} = \left(G|\mathcal{M}|^2 \langle m_{\beta\beta}\rangle^2\right)^{-1} \simeq 10^{27-28} \left(\frac{0.01\text{eV}}{\langle m_{\beta\beta}\rangle}\right)^2 \text{y}$$

Rev.Mod.Phys.91, 015001(2019); Rep.Prog.Phys.80, 046301(2017); Ann.Rev.Nucl.Part.Sci.69, 219(2019)

Unique isobar ^{96}Ru and ^{96}Zr Collisions

^{96}Ru+^{96}Ru and ^{96}Zr+^{96}Zr at $\sqrt{s_{NN}}$ =200 GeV

- A key question for any HI observable $\mathcal{O}$:

$$\frac{\mathcal{O}_{^{96}\mathrm{Ru}} + \mathcal{O}_{^{96}\mathrm{Ru}}}{\mathcal{O}_{^{96}\mathrm{Zr}} + \mathcal{O}_{^{96}\mathrm{Zr}}} \stackrel{?}{=} 1$$

- Expectation:

Deviation from 1 could have an origin in the nuclear structure, which impacts the initial state and then survives to the final state.

$$\mathcal{O} \approx b_0 + b_1\beta_2^2 + b_2\beta_3^2 + b_3(R_0 - R_{0,\mathrm{ref}}) + b_4(a - a_{\mathrm{ref}})$$

^{96}Ru ^{96}Ru

Quadrupole

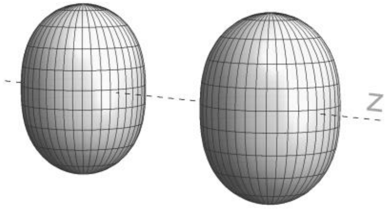

$$R_{\mathcal{O}} \equiv \frac{\mathcal{O}_{\mathrm{Ru}}}{\mathcal{O}_{\mathrm{Zr}}} \approx 1 + c_1\Delta\beta_2^2 + c_2\Delta\beta_3^2 + c_3\Delta R_0 + c_4\Delta a$$

Only probe structure differences

^{96}Zr ^{96}Zr

Pear-shaped nuclei

Octupole

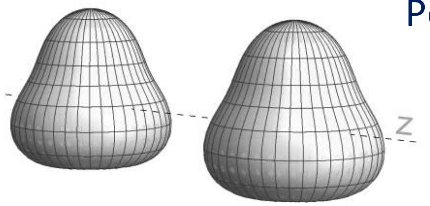

Species	β_2	β_3	a_0	R_0
Ru	0.162	0	0.46 fm	5.09 fm
Zr	0.06	0.20	0.52 fm	5.02 fm
difference	$\Delta\beta_2^2$	$\Delta\beta_3^2$	Δa_0	ΔR_0
	0.0226	-0.04	-0.06 fm	0.07 fm

Relate to neutron skin: $\Delta r_{\mathrm{np}} = \langle r_n \rangle^{1/2} - \langle r_p \rangle^{1/2}$

$$\Delta r_{np,\mathrm{Ru}} - \Delta r_{np,\mathrm{Zr}} \propto \underbrace{(R_0\Delta R_0 - \overbrace{R_{0p}\Delta R_{0p}) + 7/3\pi^2(a\Delta a}^{\text{charge}} - a_p\Delta a_p)}_{\text{mass}}$$

Model: C. Zhang and J. Jia, PRL128, 022301(2022); J. Jia and C. Zhang, PRC107, L021901(2023);
J. Jia, G. Giacalone and C. Zhang, PRL131, 022301(2023)

Nuclear structure via v_n ratio

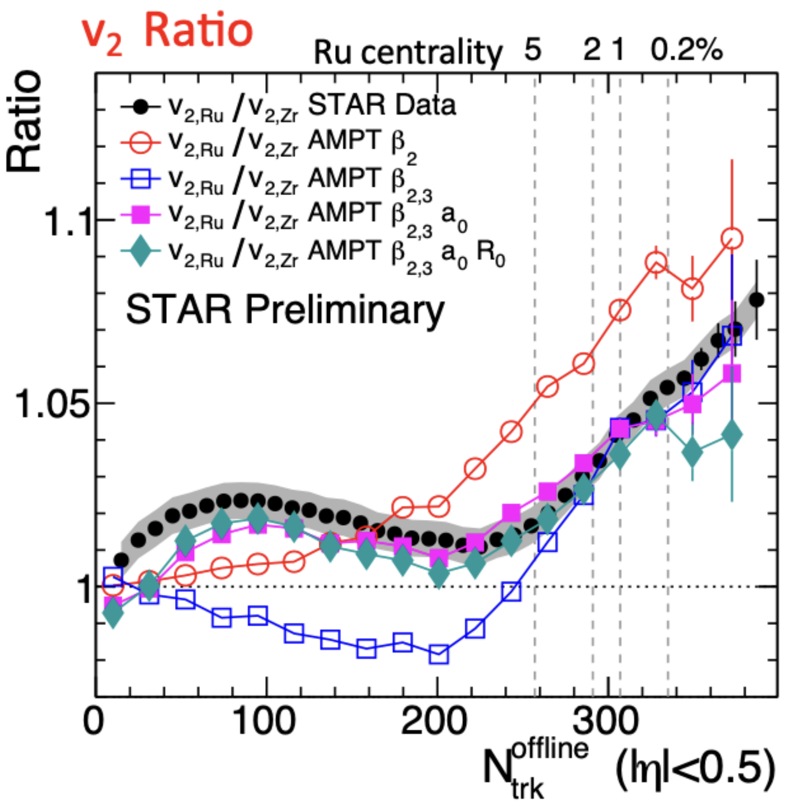

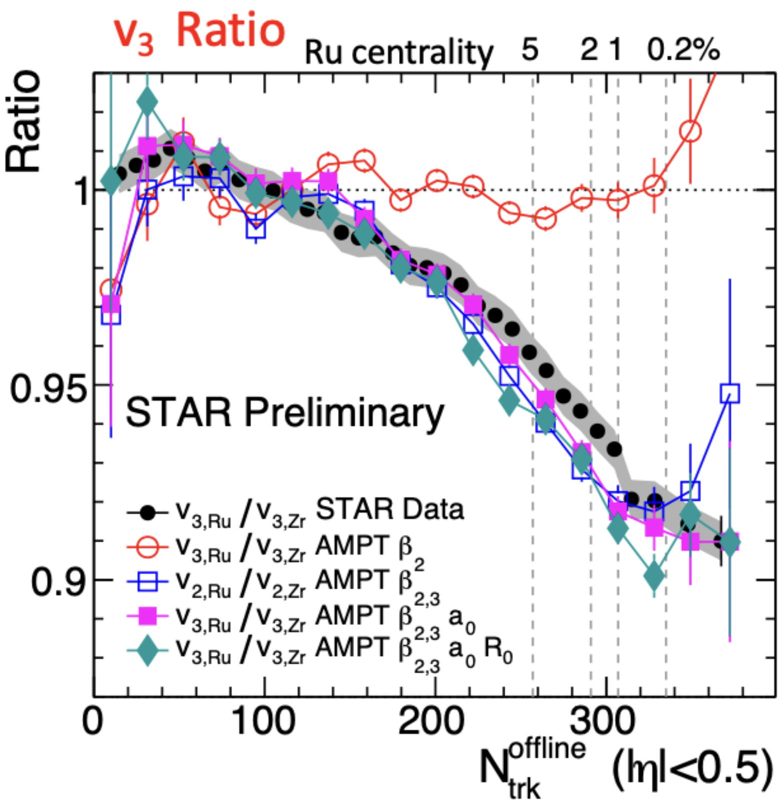

- β_{2Ru} ~ 0.16 increase v_2, no influence on v_3 ratio
- β_{3Zr} ~ 0.2 decrease v_2 in mid-central, decrease v_3 ratio
- Δa_0 = -0.06 fm increase v_2 mid-central, small impact on v_3
- Radius ΔR_0 = 0.07 fm only slightly affects v_2 and v_3 ratio.

- Direct observation of octupole deformation in ^{96}Zr nucleus
- Clearly imply the neutron skin difference between ^{96}Ru and ^{96}Zr
- Simultaneously constrain these parameters using different N_{ch} regions

Nuclear structure influences everywhere

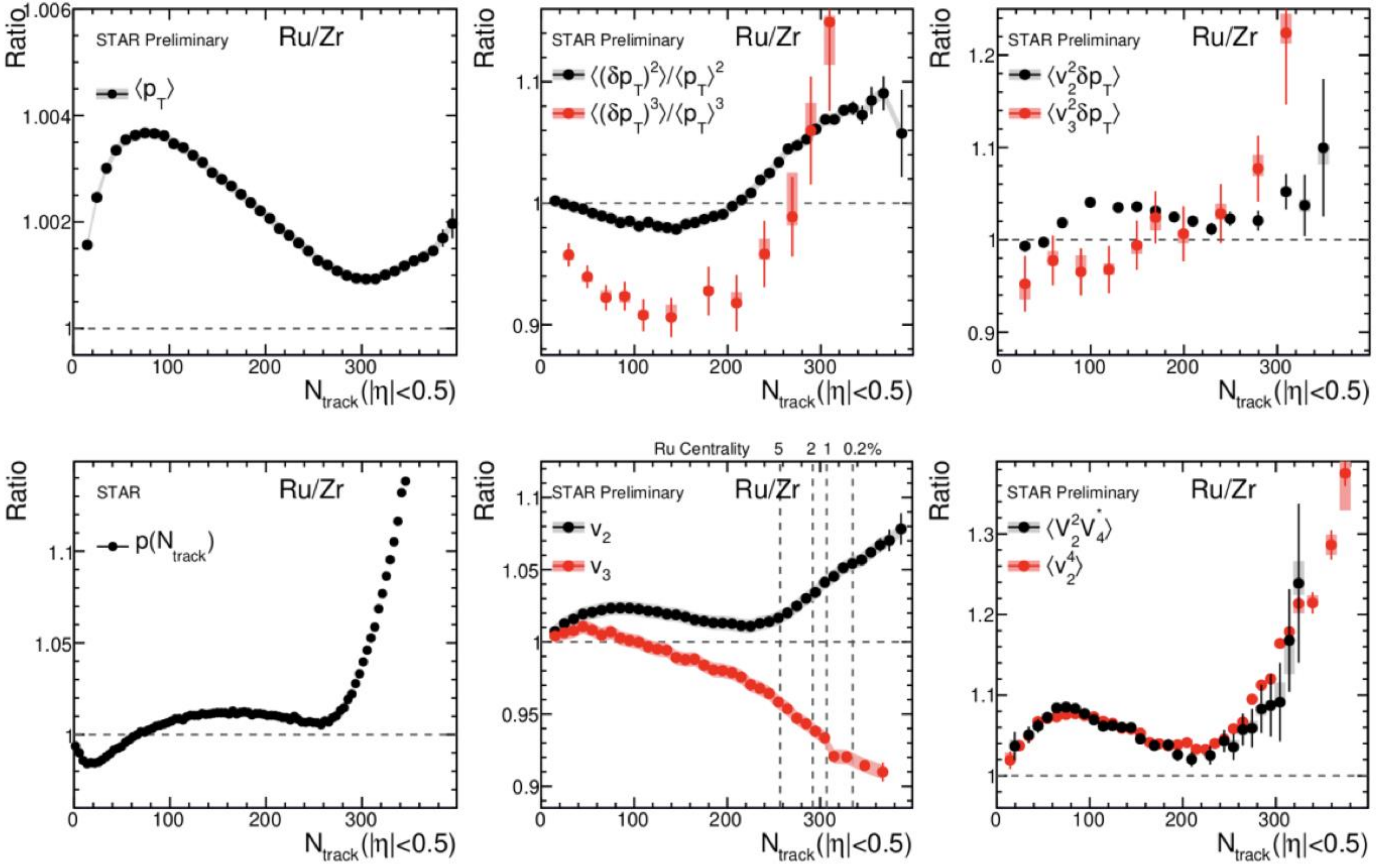

Isobar ratios cancel final state effect

- Vary the shear viscosity by changing partonic cross-section
  - Flow signal change by 30-50%, the v_n ratio unchanged.

C. Zhang, S. Bhatta and J. Jia, PRC106, L031901(2022)

$$v_n = k_n \varepsilon_n$$

$$\frac{v_{n,\mathrm{Ru}}}{v_{n,\mathrm{Zr}}} \approx \frac{\varepsilon_{n,\mathrm{Ru}}}{\varepsilon_{n,\mathrm{Zr}}}$$

Robust probe of initial state!

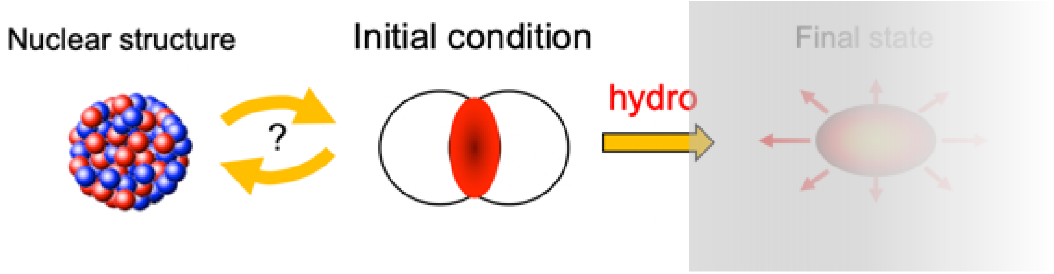

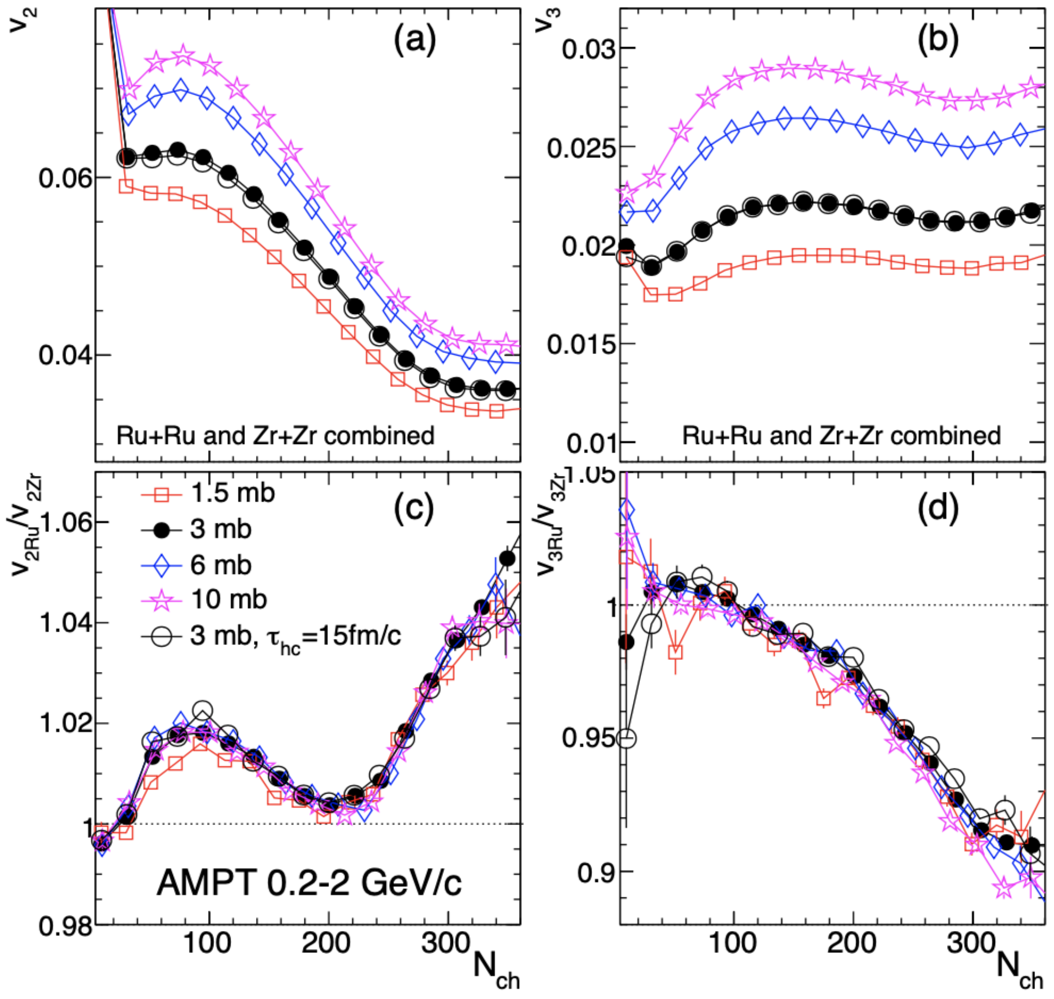

IV. Benchmarking tomography of many-body correlation in light ^{16}O nucleus

--- from one-body distribution to many-body nucleon correlations

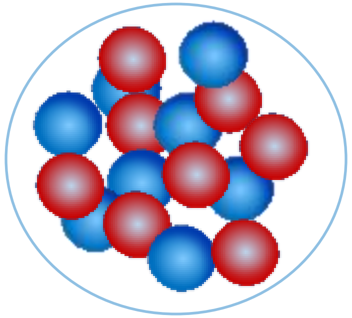

$$\rho(r) \propto \frac{1 + w\left(r^2/R^2\right)}{1 + e^{(r-R)/a_0}}$$

→ first-principle ab initio framework

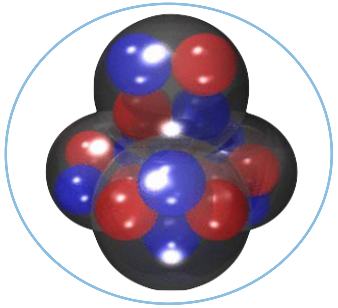

Hideki Yukawa 

“for his prediction of the existence of mesons on the basis of theoretical work on nuclear forces”

Nucleon nucleon correlations in finite quantum many-body systems

"Double magic number" in $^{16}_{8}O$ nuclei, possible cluster inside based on the low energy.

***Woods-Saxon:** without many-body nuclear correlation*

***Nuclear Lattice Effective Field theory (NLEFT):** model with many-nucleon **correlation** including α clusters*

Lu et al., PLB797, 134863(2019)
M. Freer et al., RevModPhys90, 035004(2018)
S. Elhatisari et al. Nature 630, 59 (2024)
Calculations from Dean Lee

Variational auxiliary field diffusion Monte Carlo (VMC):

MC solution of Schrödinger eq. from the time evolution of trial wave function.

A. Lonardoni et al., PRC97, 044318(2018)
J. Carlson and R. Schiavilla, RevModPhys70, 743(1998)

ab-initio Projected Generator Coordinate Method (PGCM):

Wave function from variational calculation (as in density functional theory)

Frosini et al., EPJA58, 62(2022); EPJA58, 63(2022);
EPJA58, 64(2022)
Calculations from Benjamin Bally

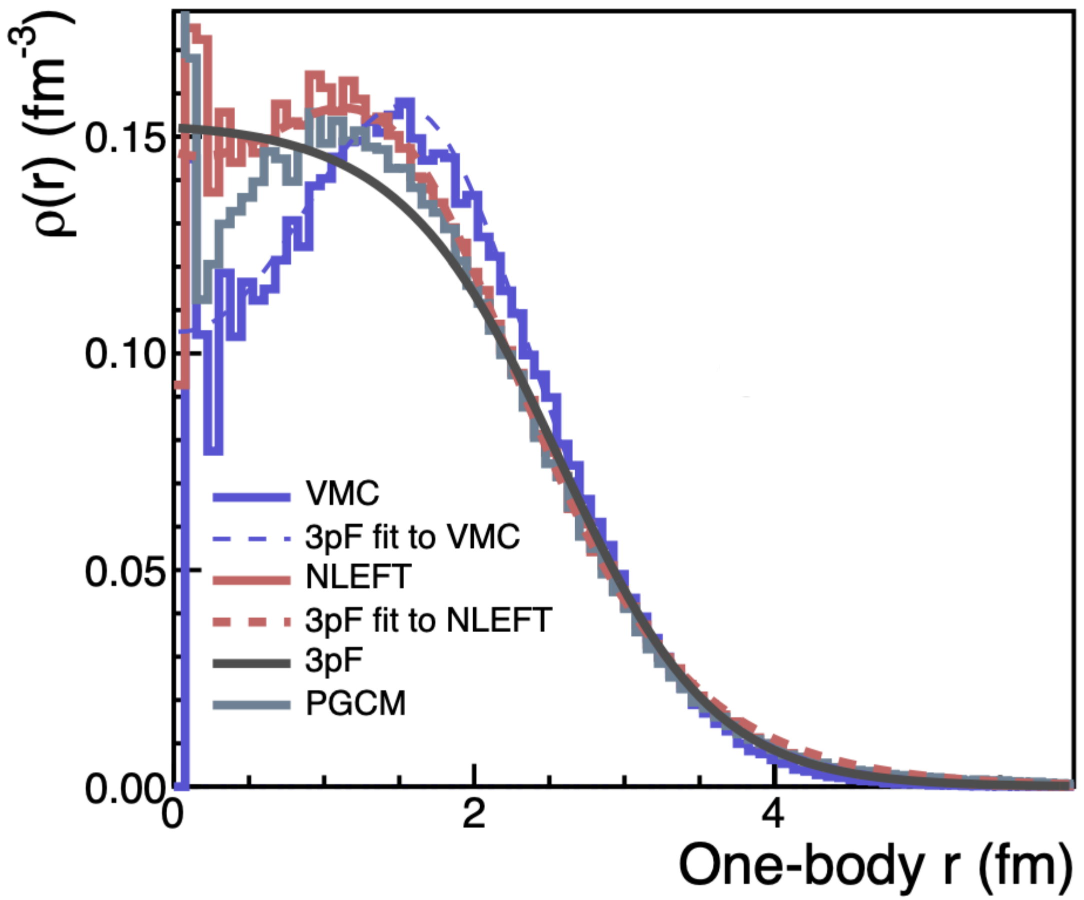

Geometric tomography of ^{16}O nucleus for the first time in high energy

O+O run2021: 600M MB and 250M HM events

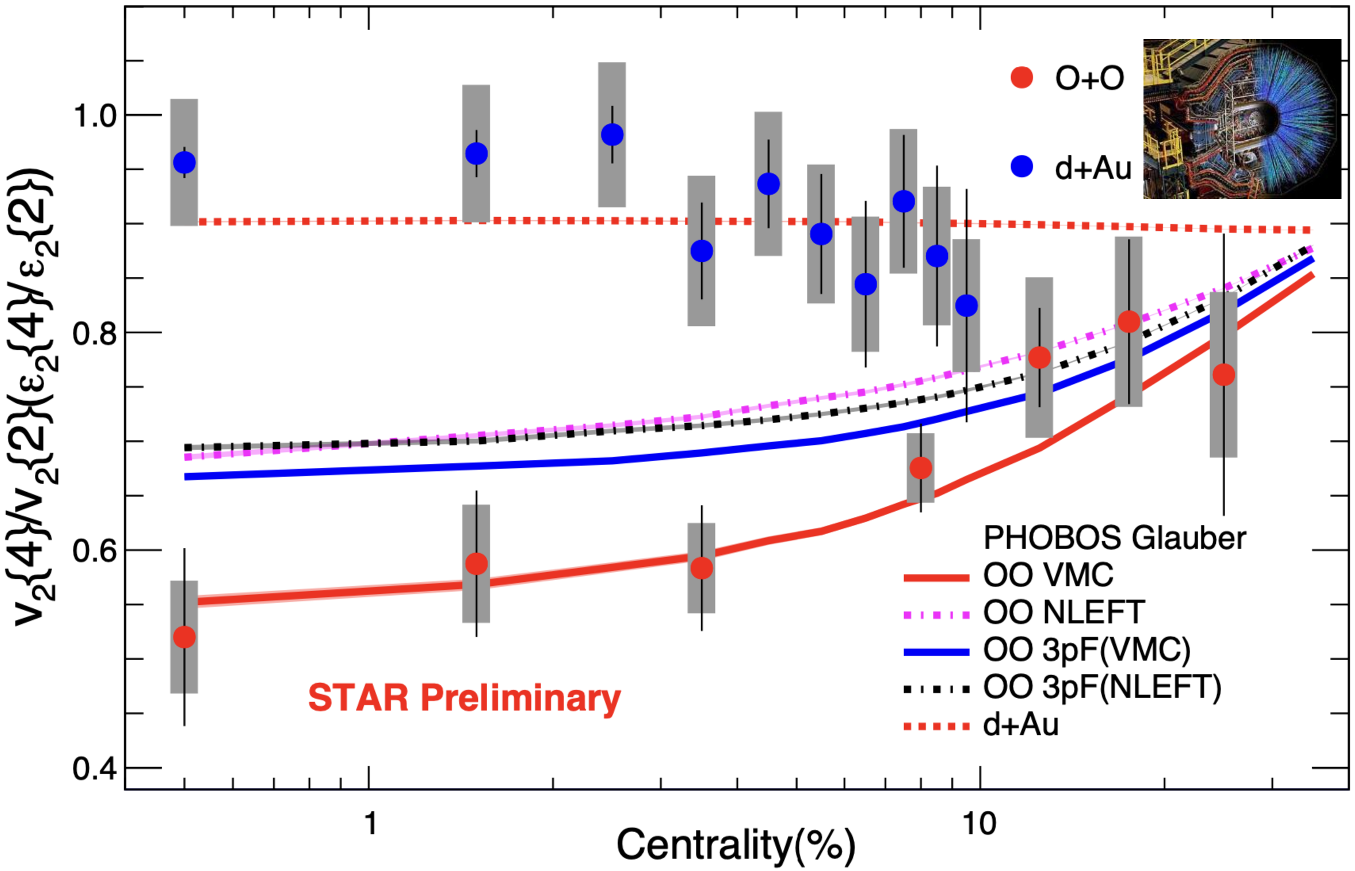

$$(v_n\{2\})^2 = c_n\{2\} = \langle v_n^2 \rangle$$
$$(v_n\{4\})^4 = -c_n\{4\} = 2\langle v_n^2 \rangle^2 - \langle v_n^4 \rangle$$

$$\varepsilon_2\{2\}^2 = \langle \varepsilon_2^2 \rangle$$
$$\varepsilon_2\{4\}^4 = 2\langle \varepsilon_2^2 \rangle^2 - \langle \varepsilon_2^4 \rangle$$

$\varepsilon_2\{4\}/\varepsilon_2\{2\}$ from three models:

1. WS is away from STAR data.

2. VMC and EFT have a visible difference.

Can many-nucleon correlations significantly impact the eccentricity fluctuations? YES!

VMC and EFT theory have visible differences describing the $v_2\{4\}/v_2\{2\}$. The interplay between sub-nucleon fluctuation and many-nucleon correlation.

STAR, PRL130, 242301(2023)

Geometric scan elucidates nuclear tomography and **strong nuclear force?**

O+O and p+O at LHC Run2025 possible Ne+Ne collisions?

Model: C. Zhang, J. Chen, G. Giacalone, S. Huang, J. Jia and Y. Ma, 2404.08385;
G. Giacalone, B. Bally, G. Nijs et al., 2402.05995; X. Zhao, G. Ma. Y. Zhou, Z. Lin and C. Zhang, 2404.09780;
Y. Wang, S. Zhao, B. Cao, H. Xu and H. Song, PRC109, L051904(2024)

V. Conclusions and Outlooks

1. Understanding nuclear structure is crucial for nucleosynthesis, nuclear fission, and neutrinoless double beta decay et al.

2. As a novel tool to unveil nuclear structure, also could help better treat QGP initial conditions further understand fundamental structure in odd- or even-nuclei.

3. Decoding the nuclear structure utilizing many bulk tools via vast final state hadrons.

4. The signatures of nuclear structure in heavy-ion collisions are everywhere, robust and reliable:
   ---constrain quadrupole deformations but also observe a slight triaxiality shape in ^{238}U

$$\beta_{2\mathrm{U}} = 0.297 \pm 0.013 \qquad \gamma_U = 8.6^\circ \pm 4.8^\circ$$

5. Heavy ion collisions open the interdisciplinary connection between low- and high-energy.
   ---octupole and hexadecapole nuclear deformations, rigid and soft triaxiality, neutron skin, nuclear cluster in light nuclei

Expect more collaborations for understanding the nature of the shape of atomic nuclei!

Thank you!

Low energy community

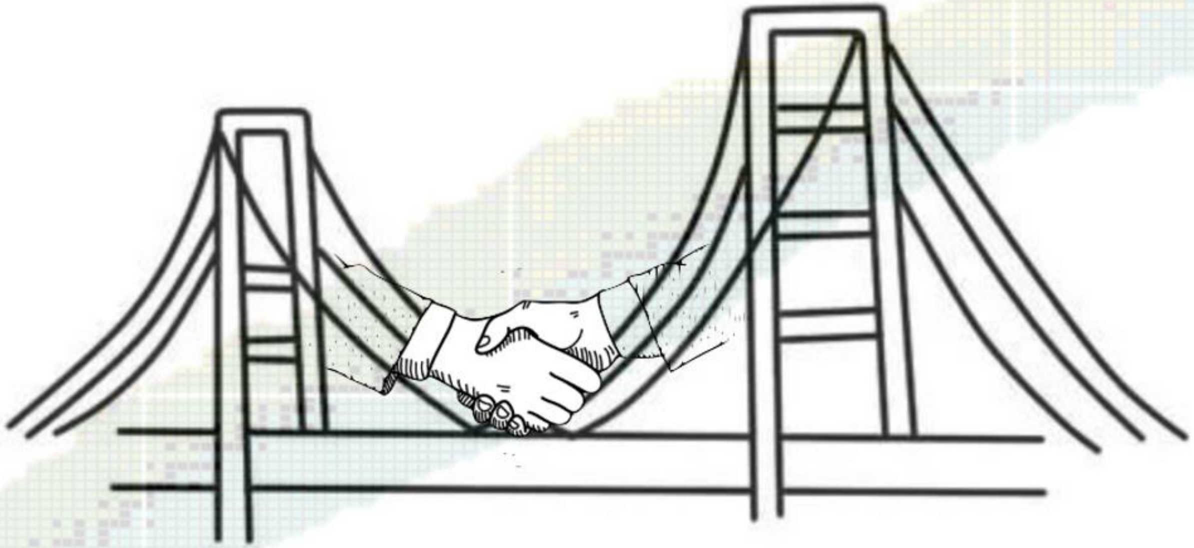

High energy community

I apologize I may not have enough time to cover all the important other studies...

Backup

Connecting the initial conditions to the nuclear shape

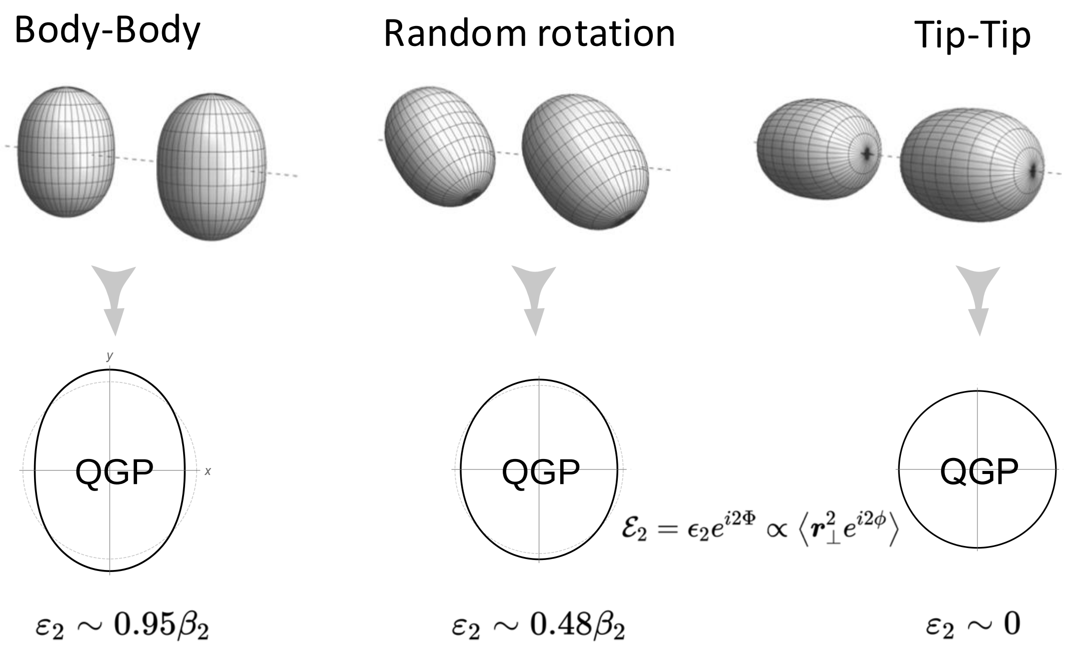

$$\rho(r,\theta,\phi) = \frac{\rho_0}{1+e^{(r-R(\theta,\phi))/a_0}}$$

$$R(\theta,\phi) = R_0(1+\beta_2[\cos\gamma Y_{2,0}(\theta,\phi) + \sin\gamma Y_{2,2}(\theta,\phi)] + \beta_3 Y_{3,0}(\theta,\phi))$$

- In principle, can measure any moments of $p(1/R, \varepsilon_2, \varepsilon_3 ...)$
  - Mean $\langle d_\perp \rangle$
  - Variance $\langle \varepsilon_n^2 \rangle$, $\left\langle (\delta d_\perp/d_\perp)^2 \right\rangle$
  - Skewness $\langle \varepsilon_n^2 \delta d_\perp/d_\perp \rangle$, $\left\langle (\delta d_\perp/d_\perp)^3 \right\rangle$
  - Kurtosis $\langle \varepsilon_n^4 \rangle - 2\langle \varepsilon_n^2 \rangle^2$, $\left\langle (\delta d_\perp/d_\perp)^4 \right\rangle - 3\left\langle (\delta d_\perp/d_\perp)^2 \right\rangle^2$
- All have a simple connection to deformation
  - Two-points correlation
  - Three-points correlation

$$\boldsymbol{\epsilon}_2 = \underbrace{\boldsymbol{\epsilon}_0}_{\text{undeformed}} + \underbrace{\boldsymbol{p}(\Omega_1,\Omega_2)}_{\text{phase factor}}\beta_2 + \mathcal{O}(\beta_2^2)$$

Shape depends on Euler angle Ω=ϕθψ

$$\left\langle \epsilon_2^2 \right\rangle \approx \left\langle \epsilon_0^2 \right\rangle + 0.2\beta_2^2$$

$$\left\langle v_n^2 \right\rangle \propto \left\langle \epsilon_n^2 \right\rangle$$

$$\left\langle \varepsilon_2^2 \right\rangle \sim a_2 + b_{2,2}\left\langle \beta_2^2 \right\rangle + b_{2,3}\left\langle \beta_3^2 \right\rangle$$
$$\left\langle \varepsilon_3^2 \right\rangle \sim a_3 + b_{3,3}\left\langle \beta_3^2 \right\rangle + b_{3,4}\left\langle \beta_4^2 \right\rangle$$
$$\left\langle \varepsilon_4^2 \right\rangle \sim a_4 + b_{4,4}\left\langle \beta_4^2 \right\rangle$$
$$\left\langle (\delta d_\perp/d_\perp)^2 \right\rangle \sim a_0 + b_0\beta_2^2 + b_{0,3}\beta_3^2$$

$$\left\langle \varepsilon_2^2 \delta d_\perp/d_\perp \right\rangle \sim a_1 - b_1\cos(3\gamma)\beta_2^3$$
$$\left\langle (\delta d_\perp/d_\perp)^3 \right\rangle \sim a_2 - b_2\cos(3\gamma)\beta_2^3$$

J. Jia, PRC105, 014905(2022)